important in both physiological and pathological conditions in the liver [22]. The reconstructed sinusoidal structures between the h-hepatocytes and m-stellate cells were immunohistologically visualized by staining of these two types of cells with antibodies against h-CK8/18 and m-desmin, respectively (**Figure 2**). Our results indicate that the livers of the chimeric mice with a high RI consisted of parenchymal cells (mostly h-cells and a small percentage of m-cells), m-nonparenchymal cells and m-ECMs. Therefore, it is apparent that xenogeneic interactions between the h-parenchymal and m-nonparenchymal liver cells supported the construction of an m-liver that was seemingly normal in terms of histological structure and biochemical function. Meuleman *et al.* [21] showed the formation of functional bile canaliculi connected to mouse canaliculi by electron microscopy. There was a good correlation between the RI and mRNA expression levels of such housekeeping genes as hAlb and h-transferrin, supporting the notion that transplanted h-hepatocytes were functional [23]. In our experience, mice with > 6 mg/ml hAlb in their blood have an RI > 70%.

That h-hepatocytes are accepted by the m-nonparenchymal community and are able to construct a liver that biochemically and morphologically resembles an m-liver and is capable of supporting mouse life indicates that basic features of hepatocytes are common to humans and mice, despite the big species difference.

Many hepatocyte proteins are required to support the growth and maintenance of a mouse, and h-hepatocyte proteins appear to be functionally recognized as m-hepatocyte proteins in mice. We suggest that h-hepatocytes are able to express most h-proteins even in the quite different m-liver environment. That is, the autonomy of h-hepatocytes is maintained in a xenogeneic environment under immunotolerant conditions. It appears that h-hepatocytes can keep their autonomy as h-hepatocytes in an m-liver without disrupting the life of the mouse, at least for the time periods studied (up to 80 days after transplantation). This conclusion is our rationale for the use of h-hepatocyte-chimeric mice as an experimental tool for studying the biology and pharmacology of h-hepatocytes. However, many details of this supposition remain to be demonstrated experimentally.

7. Infection of a chimeric m-liver with human hepatitis viruses and the propagation thereof

The infectivity of human-specific viruses, such as hepatitis B virus (HBV) and HCV, in h/m-chimeric mice and the propagation of such viruses provides a criterion for determining whether the chimeric m-liver is 'humanized'. Additionally, if these mice are sensitive to such viruses, they may be useful as infectious disease animal models, because human liver diseases caused by HBV and HCV have been studied extensively worldwide in the search for effective antiviral medicines [24]. Moreover, rodents are not useful animal models, due to the strict species specificity of viruses [25]. Further, h-hepatocytes in culture are not sensitive to such viruses.

Two groups sought to inoculate chimeric mice with hepatitis virus-infected h-serum. They found that the h/m-chimeric mice were not only infected by the viruses, but could also be hosts for viral propagation; one for HBV, using h-hepatocyte-chimeric Rug-2-knockout mice [13], and the other for HCV, using h/m-chimeric uPA/SCID mice [14]. In the HCV infection study, the homozygous animals were superior to their hemizygous counterparts, due to a substantial advantage in terms of the magnitude and duration of h-hepatocyte engraftment in the former. Viral replication was confirmed by the detection of negative-strand viral RNA in the transplanted livers. HCV proteins were localized to h-hepatocyte colonies, and the infection was serially passaged through three generations of mice, confirming both the synthesis and release of infectious viral particles.

Subsequently, we also assessed the infectivity of HBV in the chimeric mice [26]. The mice were inoculated with h-serum containing HBV. High-level viremia was observed in mice inoculated with HBV-positive h-serum for up to 22 weeks. Passage experiments showed that the serum of the mice contained infectious HBV. As in the case of the HCV infection study, the degree of viremia tended to be higher in those mice with a greater RI. Further, it was demonstrated that lamivudine, an anti-HBV drug, effectively reduced the degree of viremia in the infected mice, indicating that chimeric mice are a useful model for the development and evaluation of anti-human hepatitis virus drugs.

8. Humanization of drug metabolism in the chimeric m-liver

Humans take in many natural and artificial materials from their surrounding environment, including foods, nutrients and drugs. The biochemical treatment of foreign substances, or xenobiotics, is one of the major tasks of the liver, and this is achieved somewhat differently in mice and humans. Thus, the metabolic pathway induced by a xenobiotic administered to a chimeric mouse could be an important criterion in evaluating the humanness of a chimeric m-liver. This criterion is probably also of major commercial significance with respect to the R&D of efficient and effective new drugs for humans.

Conventionally, rodents, especially rats, have been used as animal models to study the metabolism and safety of a candidate drug; if a chimeric mouse is sufficiently humanized in terms of drug metabolism, it may provide an innovative new model valuable for R&D leading to the development of new medicines. When administered, a xenobiotic is taken up largely by hepatocytes and distributed intracellularly, metabolized and secreted, via the bile or urinary duct, through the processes of absorption, distribution, metabolism, and excretion (ADME). Each step in the ADME of a drug involves multiple genes and their corresponding proteins, and is species-dependent. Further, the steps in these processes are interdependently regulated; thus, the pharmacokinetics of a drug is species-dependent, determined by parameters resulting from these interactive

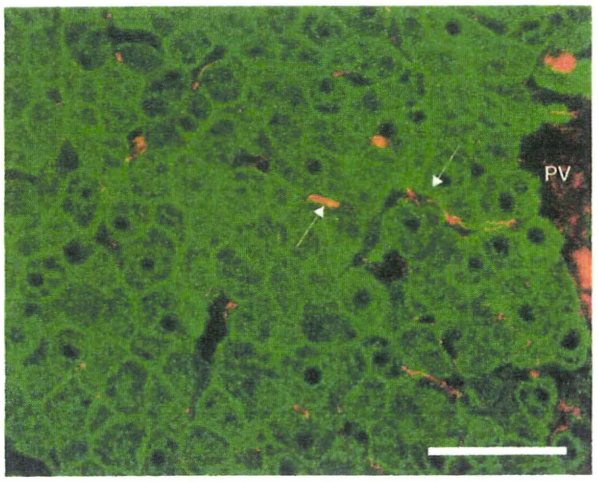

Figure 2. Chimeric sinusoids formed by the elaborate collaboration of h-hepatocytes with m-nonparenchymal cells.
A liver section prepared from a liver lobule of a chimeric mouse was double immunostained with h-CK8/18 (green) for h-hepatocytes and desmin (red) for m-stellate cells (indicated by arrows).
Bar: 10 μm.
h: Human; m: Mouse; PV: Portal vein.

processes. The potential for differences in the ADME of a drug between humans and rodents means that caution must be taken in order to correctly extrapolate the pharmacokinetics of xenobiotics in rodents to those in humans.

Xenobiotics are metabolized in hepatocytes by xenobiotic-metabolizing enzymes (XMEs) in two phases. Phase I involves oxidative enzymes while Phase II involves conjugating enzymes that create more stable, hydrophilic derivatives [27]. Drugs, toxicants and chemical carcinogens are processed in Phase I primarily by the cytochrome P450 (CYP) and flavin-containing monooxygenase superfamilies, with the former being especially important in eliminating most clinical drugs. Thus, we examined the expression profile of CYP enzymes in chimeric m-livers to assess the degree of humanization.

8.1 Phase I drug metabolism

Among the known CYP families, four families, CYP1 – 4, are known to play primary roles in xenobiotic metabolism. In particular, CYP3A4 is the most abundantly expressed CYP in human liver and metabolizes more than 60% of all therapeutic drugs [27]. CYP2D6 is also important in drug R&D; it is believed that 70% of the drugs on the market are metabolized by these two enzymes [27].

From the viewpoint of humanization, CYP isoforms CYP2C8, CYP2C9, CYP2C18 and CYP2C19 are useful targets for study because all are found in the h-liver, but are absent from m- and r-livers [28,29]. Western blot analyses using h-specific antibodies against CYP2C9 of hepatocytic microsomal fractions from h/m-chimeric mice with an RI > 34% showed positive signals, in contrast to those from chimeric mice with an RI < 28% or control mice (mice not transplanted with h-hepatocytes) [20]. CYP2C9 has diclofenac 4′-hydroxylation activity. Microsomal fractions from the chimeric mice showed diclofenac 4′-hydroxylase activity, the degree of which depended on the RI of the mouse. These positive results support our expectation that h-hepatocytes in chimeric livers retain h-type pharmacologic activity toward administered drugs.

As mentioned above, CYP2D6 metabolizes a large number of clinically used drugs [30,31], and there is a prominent difference in this CYP between mice and humans, making this enzyme a good test material for judging whether an animal model is useful and reliable for the study of h-type drug metabolism [32,33]. The CYP2D subfamily in humans has a single active member, CYP2D6. Rats and mice carry at least five genes, but none encodes a protein with the same enzymatic activity as its h-counterpart [32,34]. Debrisoquin is an h-CYP2D6 substrate that is largely metabolized to 4′-hydroxydebrisoquin in a reaction inhibited by quinidine, an h-CYP2D6 enzyme inhibitor. When debrisoquin was administered to the chimeric mice, 4′-hydroxydebrisoquin was detected in the blood of the animals, and its levels were decreased in mice pretreated with quinidine [35]. This result further suggests that the chimeric m-livers were humanized.

Additional support for the human-ness of the h-hepatocytes in the chimeric mouse livers was obtained in an experiment in which we selected six major CYP subfamilies with primary roles as XMEs, CYP1A1, 1A2, 2C9, 2C19, 2D6 and 3A4, and compared their mRNA and protein expression profiles between chimeric mouse and donor livers [20]. All of the RI-dependent mRNAs were detected. Mice with a greater RI value generally showed much stronger h-CYP expression than did mice with a lower RI value.

Our results showed that the h-hepatocytes in the chimeric mice expressed all six h-CYP genes in a semi-normal manner, as in the human body (**Figure 3**). The h-CYP1A and h-CYP3A4 subfamilies are known to specifically respond to 3-methylcholanthrene (3-MC) and rifampicin, respectively [36]. To address whether the chimeric m-livers retained the expected reactivity against these specific inducers, the mice were treated with 3-MC (**Figure 3A**) or rifampicin (**Figure 3B**). Neither 3-MC nor rifampicin induced the expression of any of the six hCYPs in uPA/SCID mice that had not been transplanted with h-hepatocytes, indicating the specificity of these inducers for h-hepatocytes [37]. 3-MC enhanced the mRNA expression of CYP1A1 and CYP1A2 10- and 6-fold, respectively, but not of the other four CYPs examined. Rifampicin enhanced the expression of h-CYP3A4 in the chimeric mice sixfold, but not of the other five hCYPs tested. Rifabutin, an analogue of rifampicin, also specifically induced h-CYP3A in the chimeric m-livers, but not murine Cyp3a [36]. The CYP3A4-induction potency in the chimeric mice is useful for drug testing because, as mentioned above, many drugs are substrates of CYP3A4 and, thus, its induction decreases the

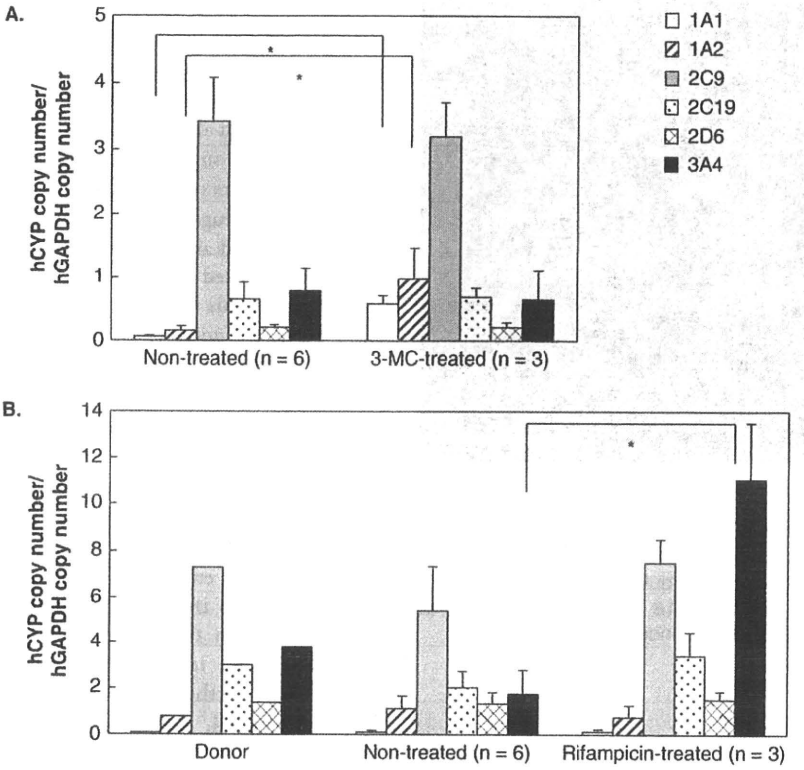

Figure 3. Expression profiles of the CYP1-3 subfamily genes in the chimeric mice. A. Chimeric mice made with h-hepatocytes from a 12-year-old boy were sacrificed ~ 70 days post-transplantation. Some mice were treated with 3-MC at 20 mg/kg body weight/day for the last 4 days. The mRNA expression of six CYP subfamilies, 1A1, 1A2, 2C9, 2C19, 2D6 and 3A4, was quantified by quantitative real-time reverse transcriptase-PCR using h-specific primers. **B.** Chimeric mice made with h-hepatocytes from a 9-month-old boy were sacrificed ~ 70 days post-transplantation. Some mice were treated with rifampicin at 50 mg/kg body weight/day for the last 4 days. Liver tissues were also obtained from the donors. The mRNA expression of six CYP subfamilies was determined as in **A.** The results shown are the average of the tested samples. Thin vertical bars indicate s.d.. The donor expression levels represent the averages of duplicate determinations for the same sample.

*Significant difference ($p < 0.01$) between the indicated measurements.

The graphs are modified from those published previously [20].

3-MC: Methylcholanthrene; h: Human.

pharmacological potency of drugs [27]. Thus, h-hepatocytes appear to be able to maintain their autonomy in an m-liver environment, at least as far as the CYPs we studied are concerned.

The specific induction of CYP by rifampicin and 3-MC in h-livers is accomplished through complex and specific cell-surface and subcellular signaling networks. Rifampicin is a ligand for pregnane X receptor (PXR), which forms a heterodimer with retinoid X receptor a (RXRa) forming a complex (rifampicin/PXR/RXRa) that upregulates CYP3A4 gene expression by binding to a xenobiotic response element composed of a direct repeat of α and β half-sites separated by four nucleotides [38]. Rifampicin is a potent activator of human and rabbit PXR, but has little activity toward rat or mouse PXR [39]. That the chimeric m-livers were responsive to rifampicin suggests that h-specific PXR/RXRa-dependent intracellular signaling is also at work in the chimeric m-livers, again supporting the notion that the liver data for the h/m-chimeric mice faithfully reflect those for humans. 3-MC is a ligand of aryl hydrocarbon receptor (AHR), and its complex with AHR (AHR/3-MC) is known to upregulate the genes CYP1A1, CYP1A2 and CYP1B1 by binding to their xenobiotic response elements together with AHR nuclear translocator [40]. Our studies suggest that these known ligand-activated receptor signaling pathways are functional in h/m-chimeric mouse livers. Although our data related to CYP expression, drug profiles and regulation by inducers and inhibitors are not comprehensive, our current opinion is that h-hepatocytes in mice do not lose their intricate intracellular signaling networks, which are specialized for h-hepatocyte drug metabolism; thus, hepatocyte-humanized mice may prove to be a useful animal model for studying the h-type signaling pathways that regulate xenobiotic-induced gene expression.

8.2 Humanization of the Phase II pathways of drug metabolism

The contribution of Phase II conjugation to the clearance of a drug is said to be ~ 30% [41]; in particular, compounds with polar groups are primarily metabolized in this way. The major hepatic Phase II enzymes in humans are UDP-glucuronosyltransferase (UGT), sulfotransferase (SULT), *N*-acetyltransferase (NAT) and glutathione *S*-transferase (GST), which are responsible for glucuronidation, sulfation, acetylation and glutathione conjugation, respectively. hUGT, hSULT, hNAT and hGST were expressed at the mRNA level while UGT2B7, SULT1E1, SULT2A1 and GSTA1 were expressed at the protein level in the chimeric m-livers, with a correlation between the level of expression and the RI of the mice [42]. The activities of related enzymes, including morphine 6-glucuronosyltransferase and estrone 3-SULT, were also detected in an RI-dependent manner. The protein contents and enzymatic activities of the Phase II-associated enzymes in chimeric m-livers with high RIs (~ 90%) were similar to those in the donor livers. We also compared the mRNA expression profiles of 26 Phase II h-enzymes, including members of the GST, SUL, NAT and UGT families, between the livers of chimeric mice with RIs between 71 and 89% and donors in a systematic and comprehensive manner [23]. All of the genes tested were detectable in the chimeric mice. Although the expression levels of the tested genes (65%) were significantly lower than in the donors (30 – 55% of the level in the donors), we suggest that the Phase II drug biotransformation is appreciably humanized in h/m-chimeric mice.

There are groups of clinically used drugs that bind to PXRs or constitutive androstane receptors. These ligand-activated PXRs and constitutive androstane receptors are involved in the regulation of some Phase II XME genes, including SULT1A and UGT1A [43] and GST and UGT1A [44,45], respectively. Considering the semi-normal expression profiles of the Phase II XME genes and proteins, it is likely that these ligand-activated transcriptional regulators are functional in h/m-chimeric m-livers; however, additional, direct analytical data are needed to confirm this.

8.3 Humanization of drug transportation

Generally, the recognition and intake of a drug and its secretion occur on and in the cell membrane and are the initial and final steps of proper drug handling by hepatocytes. Studies of humanization related to the membrane-associated aspects of drug treatment in chimeric mice are quite limited compared with humanization at the intracellular level, despite the general recognition of their physiological and pathological importance. Drug transportation in the liver is largely performed by two systems. The first, extrahepatic-to-hepatic transportation, involves transporters such as organic cation transporter 1, organic anion transporting polypeptide (OATP) 1B1 and OATP1B3. The second is hepatic-to-bile-duct transportation, and it involves, among others, adenosine 5′-triphosphate-binding cassette (ABC) proteins, including P-glycoprotein, bile salt export pump (ABCB11), breast cancer resistance protein (ABCG2) and multidrug resistance-associated protein 2 [46]. The former transporters are located on the sinusoidal membrane, and are responsible for the intake of drugs into hepatocytes, while the last are on the canalicular membrane, and are responsible for the biliary excretion of metabolites. The h-genes encoding these transport systems were preferentially expressed compared with their m-counterparts in chimeric mice with RIs > 60% [46]. Cefmetazole, a cephalosporin antibiotic, is excreted without chemical modification via urinary and biliary pathways. Humans use the former as the dominant pathway [47], whereas the latter has been demonstrated in rats [48] and mice [46]. Before receiving h-hepatocytes, the host mice excreted cefmetazole predominantly via the biliary pathway. The urinary pathway was dominant in chimeric mice with RIs > 60% [46].

We also examined the expression levels of 21 human transporter genes, including ABC and OATP, in the livers of chimeric mice and compared them with those in donor livers [23]. The chimeric mouse:human expression ratio for 62% of the 21 genes tested in the chimeric livers ranged from 0.35 to 0.75. We also found that when treated with fibrates, amphipathic carboxylic acids used to treat metabolic disorders and as hypolipidemic agents, the expression of multidrug-resistance P-glycoprotein 3 in the chimeric mice increased [49]. Although data related to the drug transporters in chimeric m-livers are limited, the available data suggest that chimeric livers are substantially humanized and could be useful for investigating h-type drug transport systems in drug R&D.

9. Expert opinion

To researchers who recognize the value of a liver-humanized mouse in predicting the metabolic pathway and safety of a drug in h-livers, information concerning the ADME profiles of various drugs is of great importance. To date, h-hepatocyte-chimeric mice have been largely evaluated in relation to the 'M' (CYP-associated metabolism) of ADME. It should also be remembered that most chimeric mouse-associated studies have considered these mice to be an innovative and useful *in vivo* animal model for studying the mechanisms of infection and propagation by human hepatitis viruses, for comparing the infectious potential of viral subtypes and for the screening of candidate antiviral drugs. Since the introduction of liver-humanized mice to the research environment, almost a decade has passed. During this time, interest in using chimeric mice as *in vivo* model for examining the ADME of drugs, in place of humans and conventional rodents, has gradually increased because researchers in the drug-hunting field increasingly are appreciating their usefulness. Based on our accumulated experience, we propose that these mice are significantly and appreciably humanized in terms of their hepatic phenotype (at least in terms of the factors we have examined thus far) and, thus, that the mice represent a reliable and promising animal model that may be more useful in predicting the

metabolism and efficacy of a drug in humans than any other currently available model. In chimeric mice, the liver is largely occupied by h-hepatocytes; however, it retains its structural and functional integrity as a liver while the h-hepatocytes retain their autonomy in the murine hepatic environment. Accordingly, researchers can investigate the response to a drug as if they are working with an h-liver, without being limited to just one or a few related genes or proteins, as in an h-gene-targeted Tg mouse model.

However, we are still in an initial stage of scientific characterization of chimeric mice from various aspects of interest. Above all, human pharmacokinetic scalability of the humanized mouse is one of major themes that has not been systematically studied yet, but should be extensively examined, because allometric scaling has been generally used in the prediction of human pharmacokinetics from animal species. Practically, information on drug–drug interactions estimated by, for example, changes in 'area under the curve', is essential for developing new medicines in laboratories, but has been still poor in public. The accumulations of more experience and experimental data will reveal the advantages and limitations of the hepatocyte-humanized mouse.

In commercial R&D activities for effective drug discovery, a large number of homogeneous small animal models with h-type metabolic activities are at once required on demand. We began the large-scale production of homogenous populations of hepatocyte-humanized mice with high RIs 5 years ago to meet the need for high-throughput models in drug discovery. The product mice will facilitate academic and industrial research activities aimed at examining the h-type metabolism of new drugs and the mechanism of h-HCV infection and propagation, with the goal of discovering new anti-HCV drugs. Currently, we are able to produce about 200 chimeric mice with an RI of 70% per month. The cost for testing a drug using a humanized mouse is now much higher than that with a conventional animal, but will considerably decrease as the need increases.

Several problems specific to h-hepatocyte-chimeric mice remain. Currently, chimeric mice carry only a hepatocyte population of human origin; all other cells are of murine origin. Parenchymal cells perform their functions with the support of nonparenchymal cells. Chimeric mice lack nonparenchymal cells of human origin. Some interactions between h-parenchymal hepatocytes and m-nonparenchymal cells might proceed as they normally would in a homogeneic situation, but others might not.

Additionally, it is known that endocrine regulation is necessary for hepatocytes to achieve normal metabolic homeostasis and to reestablish normal conditions when metabolic parameters move outside the normal range due to endogenous or exogenous causes. The chimeric livers are under the influence of the murine endocrine system. However, it is known that some m-hormones, such as growth hormone (GH), are not able to act on h-cells, due to an inability to form a hormone-receptor complex between mGH and h-hepatocytes [50]. Consistent with this, h-hepatocytes repopulated the host livers at about a sixfold higher rate than in the control mouse livers when the animals were given hGH. The expression of such liver growth-associated human genes as IGF-1, STAT-3, Cdc 25A and cyclin D1 was enhanced. This simple experiment explicitly demonstrates that h-hepatocytes are under GH-deficient conditions, which is obviously not physiological. If we are concerned only with GH deficiency, we can solve this problem simply by treating the chimeric mice so as to establish a physiological concentration of hGH. However, it is also apparent that there are other conditions and factors that distinguish the h-hepatocytes in chimeric m-livers from authentic h-hepatocytes.

We are entering a time when h-liver-chimeric mice will be much improved and their h-hepatocytes will be able to more fully express authentic h-hepatocyte phenotypes. This next generation of chimeric mice will facilitate research activities with both medical and pharmaceutical purposes, adding to our understanding of human hepatitis-induced diseases and speeding up the discovery of new drugs. They will also bolster our awareness of the uniqueness and similarities between h-hepatocytes and those of other mammals.

Declaration of interest

We have had two independent and nearly overlapping occasions to provide an overview of our studies and experiences with human liver-chimeric mice. The two articles share considerable content, although we have managed to distinguish the viewpoint of this article from the other (submitted to *PPAR Research*).

Our study of chimeric mice with livers composed of human and rat hepatocytes was supported by the joint program of the Yoshizato Project in Cooperative Link of Unique Science and Technology for Economy Revitalization (CLUSTER) of the Japanese Ministry of Education, Culture, Sports, Science and Technology (2002 – 2009); by the Hiroshima Prefecture and Hiroshima University 21st Century COE Program for Advanced Radiation Casualty Medicine (2003 – 2008); and by a Research on Advanced Medical Technology, Health and Labor Sciences research grant from the Ministry of Health, Labor and Welfare of Japan (2001 – 2004).

Bibliography

Papers of special note have been highlighted as either of interest (•) or of considerable interest (••) to readers.

1. Zarnegar R, DeFrances MC, Michalopoulos GK. Hepatocyte growth factor. In: Arias IM, chief editor, The Liver. Raven Press, New York; 1994. p. 1047-57
2. Tsanev R. Cell cycle and liver function. In: Reiner J, Holzer H, editors, Results and Problems in Cell Differentiation. Springer-Verlag, Berlin; 1975. p. 197-248
3. Stahl WR. Organ weights in primates and other mammals. Science 1965;150:1039-42
4. Thiel V, Gavaler DH, Kam JS, et al. Rapid growth of an intact human liver transplanted into a recipient larger than the donor. Gastroenterology 1987;93:1414-19
5. Heckel JL, Sandgren EP, Dege JL, et al. Neonatal bleeding in transgenic mice expressing urokinase-type plasminogen activator. Cell 1990;62:447-56
6. Mohammed FF, Pennington CJ, Kassiri Z, et al. Metalloproteinase inhibitor TIMP-1 affects hepatocyte cell cycle via HGF activation in murine liver regeneration. Hepatology 2005;41:857-67
7. Sandgren EP, Palmiter RD, Heckel JL, et al. Complete hepatic regeneration after somatic deletion of an albumin-plasminogen activator transgene. Cell 1991;66:245-56

• **The first report of hepatocyte repopulation in liver injured mouse.**

8. Sandgren EP, Degen JL, Palmiter RD, et al. Replacement of diseased mouse liver by hepatic cell transplantation. Science 1994;263:1149-52
9. Marongiu F, Doratiotto S, Montisci S, et al. Liver repopulation and carcinogenesis: two sides of the same coin? Am J Pathol 2008;172:649-857
10. Rhim JA, Sandgren EP, Palmiter RD, et al. Complete reconstitution of mouse liver with xenogeneic hepatocytes. Proc Natl Acad Sci USA 1995;92:4942-6

•• **The first report of repopulation of xenogeneic hepatocytes in mouse liver.**

11. Michalopoulos GK. Liver regeneration. J Cell Physiol 2007;213:286-300
12. Petersen J, Dandri M, Gupta S, et al. Liver repopulation with xenogeneic hepatocytes in B and T cell-deficient mice leads to chronic hepadnavirus infection and clonal growth of hepatocellular carcinoma. Proc Natl Acad Sci USA 1998;95:310-5
13. Dandri M, Burda MR, Török E, et al. Repopulation of mouse liver with human hepatocytes and in vivo infection with hepatitis B virus. Hepatology 2001;33:981-8

• **The first report on HBV infectivity in liver-humanized mouse.**

14. Mercer DF, Schiller DE, Elliott JF, et al. Hepatitis C virus replication in mice with chimeric human livers. Nat Med 2001;7:927-33

•• **The first report on HCV infectivity in liver-humanized mouse.**

15. Bosma GC, Custer RP, Bosma MJ. A severe combined immunodeficiency mutation in the mouse. Nature 1983;301:527-30
16. Perryman LE. Molecular pathology of severe combined immunodeficiency in mice, horses, and dogs. Vet Pathol 2004;41:95-100
17. Suemizu H, Hasegawa M, Kawai K, et al. Establishment of a humanized model of liver using NOD/Shi-scid IL2Rgnull mice. Biochem Biophys Res Commun 2008;377:248-52
18. Kikutani H, Makino S. The murine autoimmune diabetes model: NOD and related strains. Adv Immunol 1992;51:285-322
19. Ohbo K, Suda T, Hashiyama M, et al. Modulation of hematopoiesis in mice with a truncated mutant of the interleukin-2 receptor gamma chain. Blood 1996;87:956-67
20. Tateno C, Yoshizane Y, Saito N, et al. Near completely humanized liver in mice shows human-type metabolic responses to drugs. Am J Pathol 2004;165:901-12

•• **The first report on generating hepatocyte-humanized mice with high replacement ratio that show human-type drug metabolism.**

21. Meuleman P, Libbrecht L, De Vos R, et al. Morphological and biochemical characterization of a human liver in a uPA-SCID mouse chimera. Hepatology 2005;41:847-56
22. Kawada N, Kristensen DB, Asahina K, et al. Characterization of a stellate cell activation-associated protein (STAP) with peroxidase activity found in rat hepatic stellate cells. J Biol Chem 2001;276:25318-23
23. Nishimura M, Yoshitsugu H, Yokoi T, et al. Evaluation of mRNA expression of human drug-metabolizing enzymes and transporters in chimeric mouse with humanized liver. Xenobiotica 2005;35:877-90
24. Sarbah SA, Younossi ZM. Hepatitis C: an update on the silent epidemic. J Clin Gastroenterol 2000;30:125-43
25. Meuleman P, Leroux-Roels G. The human liver-uPA-SCID mouse: a model for the evaluation of antiviral compounds against HBV and HCV. Antivir Res 2008;80:231-8
26. Tsuge M, Hiraga N, Takaishi H, et al. Infection of human hepatocyte chimeric mouse with genetically engineered hepatitis B virus. Hepatology 2005;42:1046-54
27. Gonzalez FJ, Yu AM. Cytochrome P450 and xenobiotic receptor humanized mice. Ann Rev Pharmacol Toxicol 2006;46:41-64
28. Hewitt NJ, Lecluyse EL, Ferguson SS. Induction of hepatic cytochrome P450 enzymes: methods, mechanisms, recommendations, and in vitro-in vivo correlations. Xenobiotica 2007;37:1196-224
29. Graham MJ, Lake BG. Induction of drug metabolism: species differences and toxicological relevance. Toxicology 2008;254:184-91
30. Zanger UM, Raimundo S, Eichelbaum M. Cytochrome P450 2D6: overview and update on pharmacology, genetics, biochemistry. Naunyn Schmiedebergs Arch Pharmacol 2004;369:23-37
31. Yu AM, Idle JR, Gonzalez FJ. Polymorphic cytochrome P450 2D6: humanized mouse model and endogenous substrates. Drug Metab Rev 2004;36:243-77
32. Bogaards JJ, Bertrand M, Jackson P, et al. Determining the best animal model for human cytochrome P450 activities: a comparison of mouse, rat, rabbit, dog, micropig, monkey and man. Xenobiotica 2000;30:1131-52
33. Caldwell J. The current status of attempts to predict species differences in drug metabolism. Drug Metab Rev 1981;12:221-37
34. Masubuchi Y, Iwasa T, Hosokawa S, et al. Selective deficiency of debrisoquine 4-hydroxylase activity in mouse liver microsomes. J Pharmacol Exp Ther 1997;282:1435-41
35. Katoh M, Sawada T, Soeno Y, et al. In vivo drug metabolism model for human cytochrome P450 enzyme using chimeric mice with humanized liver. J Pharm Sci 2007;96:428-37

36. Bowen WP, Carey JE, Miah A, et al. Measurement of cytochrome P450 gene induction in human hepatocytes using quantitative real-time reverse transcriptase-polymerase chain reaction. Drug Metab Dispos 2000;28:781-8

37. Katoh M, Matsui T, Nakajima M, et al. In vivo induction of human cytochrome P450 enzymes expressed in chimeric mice with humanized liver. Drug Metab Dispos 2005;33:754-63

38. Toriyabe T, Nagata K, Takada T, et al. Unveiling a new essential cis element for the transactivation of the CYP3A4 gene by xenobiotics. Mol Pharmacol 2009;75:677-84

39. Jones SA, Moore LB, Shenk JL, et al. The pregnane X receptor: a promiscuous xenobiotic receptor that has diverged during evolution. Mol Endocrinol 2000;14:27-39

40. Cho IJ, Kim SG. Oltipraz inhibits 3-methylcholanthrene induction of CYP1A1 by CCAAT/enhancer-binding protein activation. J Biol Chem 2003;278:44103-12

41. Bjornsson TD, Callaghan JT, Einolf HJ, et al. The conduct of in vitro and in vivo drug-drug interaction studies: a Pharmaceutical Research and Manufacturers of America (PhRMA) perspective. Drug Metab Dispos 2003;31:815-32

42. Katoh M, Matsui T, Okumura H, et al. Expression of human phase II enzymes in chimeric mice with humanized liver. Drug Metab Dispos 2005;33:1333-40

43. Xie W, Yeuh M-F, Radominska-Pandya A, et al. Control of steroid, heme, and carcinogen metabolism by nuclear pregnane X receptor and constitutive androstane receptor. Proc Natl Acad Sci USA 2003;100:4150-55

44. Kodama S, Koike C, Negishi M, et al. Nuclear receptors CAR and PXR cross talk with FOXO1 to regulate genes that encode drug-metabolizing and gluconeogenic enzymes. Mol Cell Biol 2004;24:7931-40

45. Zhang J, Huang W, Chua SS, et al. Modulation of acetaminophen-induced hepatotoxicity by the xenobiotic receptor CAR. Science 2002;298:422-4

46. Okumura H, Katoh M, Sawad T, et al. Humanization of excretory pathway in chimeric mice with humanized liver. Toxicol Sci 2007;97:533-8

47. Ko H, Novak E, Peters GR, et al. Pharmacokinetics of single-dose cefmetazole following intramuscular administration of cefmetazole sodium to healthy male volunteers. Antimicrob Agents Chemother 1989;33:508-12

48. Murakawa T, Sakamoto H, Fukada S, et al. Pharmacokinetics of ceftizoxime in animals after parenteral dosing. Antimicrob Agents Chemother 1980;17:157-64

49. Shoda J, Okada K, Inada Y, et al. Bezafibrate induces multidrug-resistance P-Glycoprotein 3 expression in cultured human hepatocytes and humanized livers of chimeric mice. Hepatol Res 2007;37:548-56

50. Masumoto N, Tateno C, Tachibana A, et al. GH enhances proliferation of human hepatocytes grafted into immunodeficient mice with damaged liver. J Endocrinol 2007;194:529-37

Affiliation

Katsutoshi Yoshizato[†1,2] & Chise Tateno[3]
[†]Author for correspondence
[1]Phoenixbio Co. Ltd.,
Academic Advisor Office,
3-4-1, Kagamiyama, Higashihiroshima,
Hiroshima 739-0016, Japan
Tel: +81 82 431 0016; Fax: +81 82 431 0017;
E-mail: katsutoshi.yoshizato@phoenixbio.co.jp
[2]Osaka City University Gradate School of Medicine,
1-4-3 Asahi-machi, Abeno-ku,
Osaka 545-8585, Japan
[3]PhoenixBio,
Kagamiyama, 3-4-1 Kagamiya,
Higashihiroshima, Hiroshima 739-0046, Japan

G-to-A Hypermutation in Hepatitis B Virus (HBV) and Clinical Course of Patients with Chronic HBV Infection

Chiemi Noguchi,[1,2] Michio Imamura,[1,2] Masataka Tsuge,[1,2] Nobuhiko Hiraga,[1,2] Nami Mori,[1,2] Daiki Miki,[1,2] Takashi Kimura,[1,2] Shoichi Takahashi,[1,2] Yoshifumi Fujimoto,[1,2] Hidenori Ochi,[2,3] Hiromi Abe,[1,3] Toshiro Maekawa,[3] Chise Tateno,[2,4] Katsutoshi Yoshizato,[2,4] and Kazuaki Chayama[1,2,3]

[1]Department of Medicine and Molecular Science, Division of Frontier Medical Science, Programs for Biomedical Research, Graduate School of Biomedical Sciences, and [2]Liver Research Project Center, Hiroshima University, Hiroshima, [3]Laboratory for Liver Diseases, Single-Nucleotide Polymorphism Research Center, the Institute of Physical and Chemical Research, Yokohama, and [4]PhoenixBio, Higashihiroshima, Japan

Background. The apolipoprotein B messenger RNA editing enzyme, catalytic polypeptide–like family of cytidine deaminases induce G-to-A hypermutation in hepatitis B virus (HBV) genomes and play a role in innate antiviral immunity. The clinical relevance of this protein family is unknown.

Methods. We analyzed 33 instances in which 17 patients with chronic HBV infection experienced >2 increases of >100 IU/L in alanine aminotransferase (ALT) level; we used a quantitative differential DNA denaturation polymerase chain reaction assay to quantify the hypermutated HBV genomes observed during 21 of these 33 increases in ALT level.

Results. Of the 9 increases in ALT level that involved a >5-fold increase (relative to basal levels) in the number of hypermutated genomes observed, 8 were associated with a >2-log reduction in plasma HBV DNA level. In contrast, a corresponding decrease in plasma HBV DNA level was observed for only 1 of the 12 increases in ALT level that did not involve an increase in the number of hypermutated genomes ($P < .001$). Hepatitis B e antigen clearance was often observed in patients who experienced an increase in the number of hypermutated genomes. Interferon treatment induced hypermutation in HBV genomes in an animal model. However, there was no apparent increase in the number of hypermutated genomes among the majority of patients who received interferon therapy, probably because the number of hypermutated genomes had already increased prior to the initiation of therapy.

Conclusion. Our results suggest that a marked increase in the number of hypermutated genomes represents a strong immunological host response against the virus and is predictive of hepatitis B e antigen clearance and plasma HBV DNA level reduction.

Despite the availability of safe and effective vaccines for >2 decades, hepatitis B virus (HBV) infection is still a global health problem. Worldwide, >2 billion people are infected with HBV, and chronic HBV infection affects ~400 million people [1, 2]. It is estimated that >500,000 people die annually because of cirrhosis and/or hepatocellular carcinoma due to HBV infection [3].

Recent reports have shown that cellular cytosine deaminase (apolipoprotein B messenger RNA [mRNA] editing enzyme, catalytic polypeptide–like 3G [APOBEC3G]), packaged in human immunodeficiency virus type 1 (HIV-1), induces G-to-A hypermutation to a nascent reverse transcript of HIV-1 and reduces the infectivity of HIV, thus contributing in part to innate antiviral activity [4–8]. HIV-1 overcomes this innate defense barrier in T cells with HIV virion infectivity factor, a protein that specifically targets APOBEC3G to proteasomal degradation [9–12]. HIV-1 can infect resting CD4 T cells in lymphoid tissues but not those circulating in peripheral blood [13–16]. Resting CD4 T cells in peripheral blood are protected from HIV infection through the action of the deaminase-active

Received 30 August 2008; accepted 6 November 2008; electronically published 28 April 2009.

Potential conflicts of interest: none reported.

Financial support: Ministry of Education, Sports, Culture and Technology and Ministry of Health, Labor and Welfare (Grants-in-Aid for scientific research and development).

Reprints or correspondence: Kazuaki Chayama, MD, Dept. of Medical and Molecular Science, Div. of Frontier Medical Science, Programs for Biomedical Research, Graduate School of Biomedical Science, Hiroshima University, 1-2-3 Kasumi, Minami-ku, Hiroshima 734-8551, Japan (chayama@hiroshima-u.ac.jp)

The Journal of Infectious Diseases 2009; 199:1599–607

0022-1899/2009/19911-0007$15.00
DOI: 10.1086/598951

Table 1. Clinical profiles of 17 patients with chronic hepatitis B virus (HBV) infection who experienced >2 increases of >100 IU/L in alanine aminotransferase (ALT) level.

Patient	Sex	Age, years	ALT level, IU/L		Plasma HBV DNA level, log copies/mL	HBV serum marker status[a]		HBV subtype	Histologic result[b]	Receipt of IFN treatment
			Minimum	Maximum		HBeAg	HBeAb			
1	M	50	26	2000	8.1	+	−	C	F2, A2	Yes
2	M	31	22	230	8.2	+	−	C	F3, A2	Yes
3	F	23	14	313	8.7	+	−	C	F2, A2	Yes
4	M	22	16	846	6.9	+	−	C	F2, A1	Yes
5	F	42	10	100	7.8	+	−	C	L	No
6	F	33	21	748	8.8	+	−	C	F2, A3	Yes
7	M	23	22	339	8.4	+	−	C	L	Yes
8	F	54	22	108	6.7	−	+	C	F2, A2	No
9	M	44	17	512	9.5	+	−	C	F2, A3	No
10	M	27	39	115	8.8	+	−	C	F1, A1	Yes
11	M	36	16	452	3.8	+	−	C	F4, A3	Yes
12	M	20	21	1295	7.2	+	−	C	F2, A2	No
13	M	36	24	481	5.7	−	+	C	F2, A2	Yes
14	M	22	20	696	5.9	+	−	C	F1, A1	Yes
15	F	24	14	1544	7.7	+	−	C	F2, A2	Yes
16	M	35	10	1618	4.7	+	−	C	F2, A1	Yes
17	M	30	21	1655	6.7	+	−	C	L	Yes

NOTE. HBeAg, HBV e antigen; HBeAb, antibody against HBV e antigen; IFN, interferon; L, liver cirrhosis.

[a] Before increase in ALT level.

[b] Histologic evaluation of chronic hepatitis by use of the scoring system of Desmet et al. [29].

APOBEC3G [17]. Recent reports have shown that interferon (IFN)–α is a potent inducer of APOBEC3G [18–21]. It has also been reported that some of the HIV restriction exerted by APOBEC3G may be independent of its cytidine deaminase activity [17, 22–24].

We and others have reported the presence of small numbers of hypermutated genomes in serum samples obtained from HBV-infected patients [25–27]. Studies using HepG2 cell lines and primary human hepatocytes showed that such hypermutation is induced by the cytidine deaminase activity of the APOBEC family of proteins [27]. In our previous study, IFN induced little hypermutation in the HBV genome [27]. However, after extensive investigation supported by development of a quantitative analysis of hypermutation, we showed that both IFN-α and IFN-γ actually increase transcription of APOBEC3G mRNA in HepG2 cell lines and induce an increase in the number of hypermutated genomes [28]. We also showed that APOBEC3G induces hypermutation in HBV and reduces HBV replication levels in the absence of the deaminase activity. Thus, APOBEC3G has dual antiviral actions against HBV and is thought to be part of the host defense mechanisms, as has been shown for HIV infection. Although it is assumed that APOBEC3G is important in the host anti-HBV defense system, little is known about the clinical importance of this enzyme, because there are no methods available for the precise quantification of small amounts of hypermutated genomes.

Using a method that can measure small amounts of hypermutated genomes (differential DNA denaturation polymerase chain reaction [3D-PCR] combined with TaqMan PCR [28]), we analyzed fluctuations in the number of hypermutated genomes observed in patients with chronic HBV infection who experienced increased alanine aminotransferase (ALT) levels. The study group included patients who received IFN treatment and patients who did not.

METHODS

Patients. From 2002 through 2006 at Hiroshima University Hospital (Hiroshima, Japan), there were 17 consecutive patients with chronic hepatitis B who experienced >2 increases of >100 IU/L in ALT level and for whom stored serum samples were available. These 17 patients were enrolled in this study, among whom 33 such increases in ALT level were observed. Thirteen of 17 patients received IFN treatment, usually during an increase in ALT level. The clinical profiles of these 17 patients are shown in table 1. Written informed consent was obtained from all patients, and the study was approved by the Hiroshima University Ethics Committee.

HBV markers. Hepatitis B e antigen and antibody against e antigen were quantified by use of enzyme immunoassay kits (Abbott Diagnostics). HBV DNA was measured by use of real-time PCR performed with the 7300 Real-Time PCR System (Applied Biosystems), in accordance with the manufacturer's instructions. The primers used for amplification were 5'-TT-

TGGGCATGGACATTGAC-3' (nt 1893–1912; nucleotide numbers are those of HBV subtype C as reported by Norder et al. [30]) and 5'-GGTGAACAATGTTCCGGAGAC-3' (nt 2029–2049). For real-time PCR, we used 25 μL of SYBR Green PCR Master Mix (Applied Biosystems) with 1 μL of the DNA solution and 200 nmol/L of each primer. The amplification conditions were as follows: 2 min at 50°C, 10 min at 95°C, followed by 40 cycles of amplification (denaturation at 95°C for 15 s and annealing and extension at 60°C for 1 min). The lower detection limit of this assay was 10^3 copies/mL.

Extraction of HBV DNA and quantitative analysis of hypermutated genomes. HBV DNA was extracted from 100-μL serum samples by use of the SMITEST DNA Extraction Kit (Genome Science Laboratories) and dissolved in 20 μL of water. Hypermutated genomes were quantified by use of TaqMan 3D-PCR performed with the 7300 Real-Time PCR System (Applied Biosystems); we used a procedure described elsewhere [28], with slight modifications. In brief, the HBV DNA fragments were amplified by use of 3D-PCR in which the denaturation temperature was set lower than usual so that only G-to-A hypermutated genomes would be amplified. The amplification conditions were as follows: activation at 95°C for 10 min; followed by initial denaturation at 89°C for 20 min, to allow nonhypermutated genomes reanneal; and 45 cycles of amplification (denaturation at 89°C for 20 s, annealing at 50°C for 30 s, and extension at 62°C for 90 s). TaqMan PCR was performed using the following primers: 5'-ACTTCAACCCCAACAMRRATCA-3' (nt 2978–2999) and 5'-AGAGYTTGKTGGAATGTKGTGGA-3' (nt 24–1), where M is A or C, R is G or A, Y is T or C, and K is G or T. The probe was a 6-carboxyfluorescein (FAM)–labeled MGB probe, 5'-(FAM)-TTAGAGGTGGAGAGATGG-(MGB)-3' (nt 3184–3167). The detection limit of hypermutated genomes was 10^2 copies/mL, and nonhypermutated genomes were not amplified by 3D-PCR [28]. The reproducibility of the assay was quite high (as indicated by the small standard deviation relative to the results of the quantitative PCR control reaction), as reported in our previous study [28].

Cell culture and transfection. HepG2 cell lines were grown in Dulbecco's modified Eagle medium supplemented with 10% (vol/vol) fetal calf serum at 37°C in 5% CO_2. Cells were seeded to semiconfluence in 6-well tissue culture plates and transfected with the plasmid pTRE-HB-wt, which contained 1.4–genome length wild-type HBV genomes [31], by calcium phosphate precipitation. Seventy-two hours after transfection, the supernatant was collected for HBV DNA quantification by real-time PCR and for quantitative analysis of G-to-A hypermutated genomes [28]. The remaining supernatant was stored at −80°C for infection experiments using human hepatocyte–chimeric mice.

Quantitative analysis of G-to-A hypermutated genomes with human hepatocyte–chimeric mice. A human hepatocyte–chimeric mouse model was developed, as described previously [32], and used in infection and IFN-treatment experiments. The human hepatocytes progressively repopulated the murine host liver and were susceptible to HBV produced in cultured cell lines [31]. All animal protocols were in accordance with the guidelines of the local animal experimentation committee. The experimental protocol was approved by the Ethics Review Committee for Animal Experimentation of the Graduate School of Biomedical Sciences, Hiroshima University. Hepatocyte-chimeric mice were inoculated with 500 μL of the supernatant produced by transiently transfected cell lines. After confirmation of high-level HBV viremia, the mice were treated with 7000 IU/g/day of IFN-α, injected intramuscularly, for 14 days (the IFN-α was a gift from Hayashibara Biochemical Labs in Okayama, Japan). Human serum albumin in mouse serum was measured with the Human Albumin ELISA Quantitation Kit (Bethyl Laboratories), used in accordance with the manufacturer's instructions.

Statistical analysis. Differences between clinical groups with respect to HBV DNA and e antigen levels were examined for statistical significance, using the Mann-Whitney *U* test. A *P* value $<.05$ was considered to indicate a statistically significant difference. All statistical analyses were performed with StatView (version 5.0; SAS Institute).

RESULTS

Clinical course of disease in patients with increased ALT levels and fluctuations in the number of hypermutated genomes. Figure 1*A*–1*D* shows clinical courses for 4 representative patients (patients 1–4 in Table 1) with chronic HBV infection who experienced increases in ALT level. We observed marked decreases in HBV DNA level in association with marked increases in hypermutated genomes (figure 1*A*–1*C*, black arrows). In contrast, there was no apparent reduction in HBV level in the absence of an increase in hypermutated genomes (1*A*–1*D*, white arrows). We also analyzed the effect of IFN therapy on the number of hypermutated genomes. In some patients, we observed an increase in the number of hypermutated genomes during IFN therapy (figure 1*B* and 1*C*) as well as a marked increase in the number of hypermutated genomes and a reduction of the virus accompanied by an increase in ALT level just after cessation of IFN therapy (1*A*–1*C*, black arrows). However, in some patients, such as patient 1 (figure 1*A*), we observed no apparent increase in the number of hypermutated genomes in response to IFN therapy. However, the number of hypermutated genomes observed in samples from this patient obtained just before the initiation of IFN therapy (996/10^6 genomes) was already higher than the baseline level (157/10^6 genomes). Samples from patient 4 (figure 1*D*) showed an increase in the number of hypermutated genomes during IFN therapy (1907/10^6 genomes), though this is less than the increase observed during natural exacerbation (12,404/10^6 genomes). In fact, there was no significant difference between IFN-treated patients and untreated patients with respect to the number of hypermutated genomes observed (data not shown). These results suggest that the host's antiviral immunity level was higher at baseline than it was after

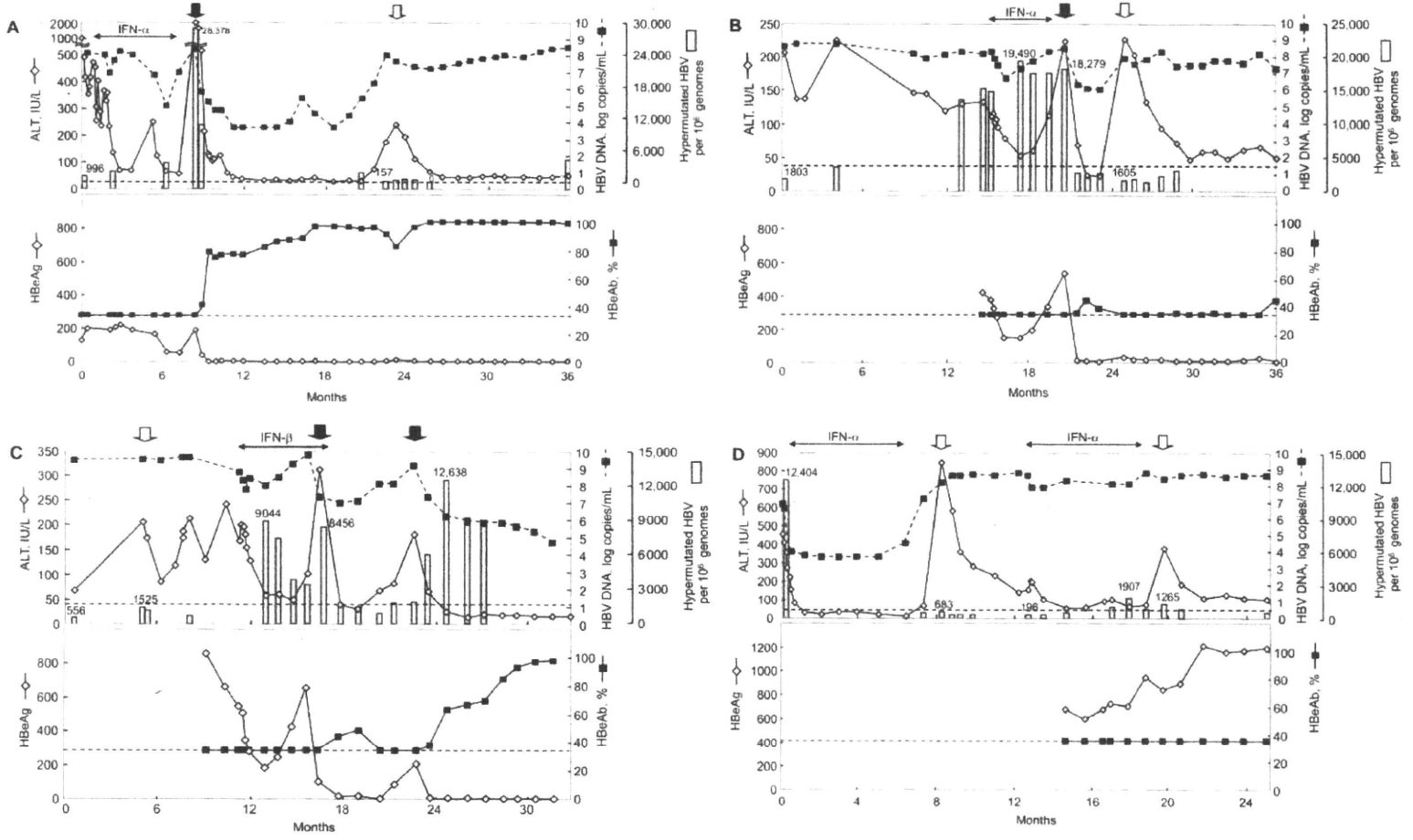

Figure 1. Clinical courses for 4 patients *(A–D)* with chronic hepatitis B virus (HBV) infection who experienced exacerbation of infection. *Black arrows,* exacerbation associated with an increase in the number of hypermutated genomes (>5 times basal levels); *white arrows,* exacerbation not associated with an increase in the number of hypermutated genomes; *horizontal dotted lines,* upper normal limit of alanine aminotransferase (ALT) (40 IU/mL; *upper panel, A–D*) and the detection limit for antibody against e antigen (HBeAb) (35%; *lower panel, A–D*). HBeAb, antibody against HBV e antigen; HBeAg, HBV e antigen; IFN, interferon.

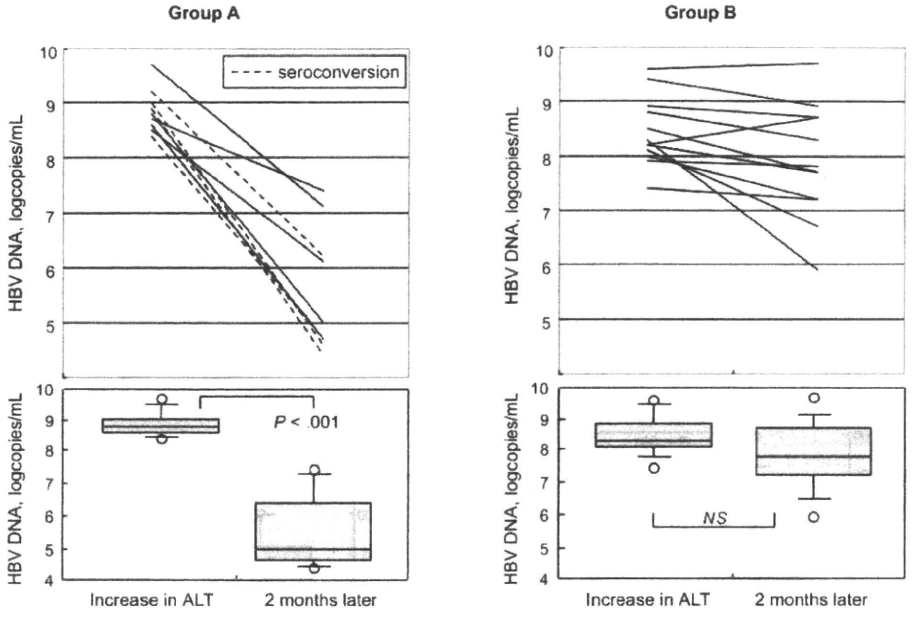

Figure 2. Relationship between increase in the number of hypermutated genomes and plasma levels of hepatitis B virus (HBV) DNA in 17 patients with chronic HBV infection who experienced >2 increases of >100 IU/L in alanine aminotransferase (ALT) level. Patients' exacerbations were divided into 2 groups, A and B, according to the extent of increase in the number of hypermutated genomes, relative to the basal number (group A included 9 exacerbations that involved a >5-fold increase in the number of hypermutated genomes; group B included 12 exacerbations that involved a ≤5-fold increase in the number of hypermutated genomes). *Upper panel* for groups A and B, individual HBV DNA levels at the time the ALT level increased and 2 months later; in the upper panel for group A, *dashed lines* indicate 4 exacerbations associated with seroconversion to positivity for antibody against e antigen. *Lower panel* for groups A and B, box-and-whisker plots for HBV DNA levels at same 2 time points. In the plots, the lines in the boxes indicate median values; the upper and lower lines of the boxes indicate the 25th and 75th percentiles, respectively; and the upper and lower whiskers represent the 90th and 10th percentiles, respectively.

IFN or that the feedback system for IFN signaling was already active before initiation of therapy.

We also compared the degree of reduction in the plasma HBV DNA level for exacerbations (i.e., increases in ALT level) associated with a marked increase in the number of hypermutated genomes (i.e., those in which the peak number was >5 times the number observed prior to exacerbation) and for exacerbations not associated with such an increase. As shown in figure 2, 8 of 9 exacerbations that were coupled with a marked increase in the number of hypermutated genomes (group A) were associated with a >2-log reduction in the HBV DNA level. In contrast, only 1 of the 12 exacerbations not associated with a marked increase in the number of hypermutated genomes (group B) was associated with a >2-log reduction in plasma HBV DNA level. The median serum HBV DNA level decreased from 8.8 to 5.0 log copies/mL among the patients in group A ($P < .001$) but did not decrease for patients in group B (figure 2).

In addition, we compared the reduction in e antigen level for these 2 groups. Levels were reduced in both groups, but the median reduction was more prominent for patients in group A than for those in group B (figure 3). All 4 exacerbations coupled with e antigen seroconversion (from positive to negative) were associated with marked increase in hypermutated genomes (figure 3).

Effect of IFN treatment on the rate of HBV hypermutation in chimeric mice. Next, we examined the effect of IFN treatment on G-to-A hypermutation in HBV genomes in human hepatocyte–chimeric mice. Two mice were intravenously injected with supernatant produced by HepG2 cells transiently transfected with a plasmid containing 1.4–genome length wild-type HBV genomes. Ten weeks later, after confirmation of high-level HBV viremia, the mice were treated with 7000 IU/g/day of IFN-α, injected intramuscularly, for 14 days. We observed an ~1.5-log reduction in plasma HBV DNA level accompanied by an increase in the number of hypermutated genomes in both mice (figure 4*A*). In a mouse inoculated with HBV but treated with phosphate-buffered saline, no increase of hypermutated genomes was observed (figure 4*B*). We also observed a 36-fold increase in the level of APOBEC3G mRNA, as determined by human oligonucleotide microarray (data not shown).

Infectivity of hypermutated genomes. To study the biological significance of hypermutated genomes, culture supernatant from HepG2 cells transfected with both HBV and APOBEC3G (5 μg each) was injected into a chimeric mouse. As shown in figure 5, the culture supernatant contained a large number of hypermutated genomes. In contrast, we could not detect hypermutated genomes in the chimeric mouse inoculated with this

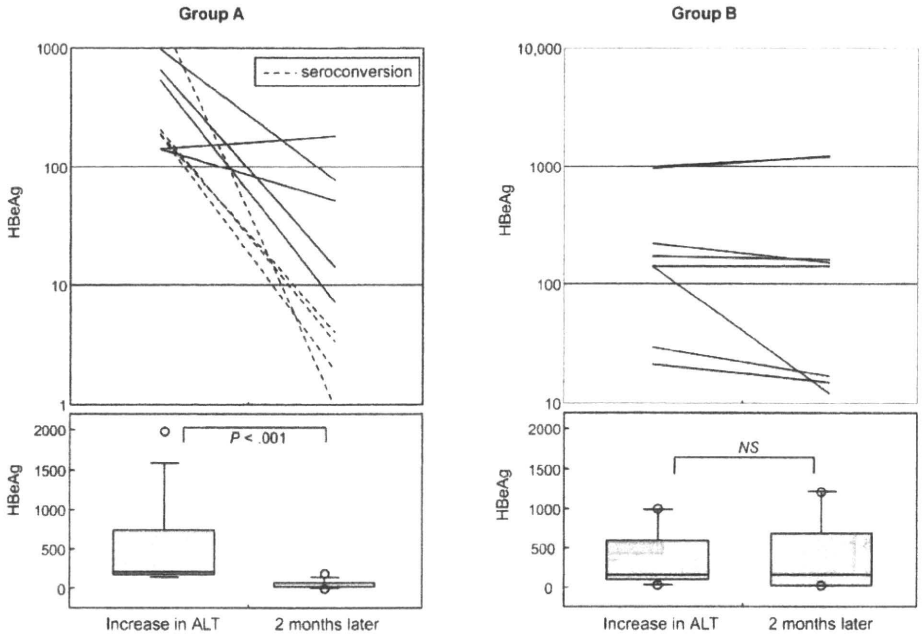

Figure 3. Relationship between increase in the number of hypermutated genomes and hepatitis B virus (HBV) e antigen (HBeAg) levels in 15 HBeAg-positive patients with chronic HBV infection who experienced >2 increases of >100 IU/L in alanine aminotransferase (ALT) level. Patients' exacerbations were divided into 2 groups, A and B, according to the extent of increase in the number of hypermutated genomes, relative to the basal number (group A included 9 exacerbations that involved a >5-fold increase in the number of hypermutated genomes; group B included 8 exacerbations that involved a ≤5-fold increase in the number of hypermutated genomes). *Upper panel* for groups A and B, individual e antigen levels at the time the ALT level increased and 2 months later; in the upper panel for group A, *dashed lines* indicate 4 exacerbations associated with seroconversion to positivity for antibody against e antigen. *Lower panel* for groups A and B, box-and-whisker plots for e antigen levels at these same 2 time points. In the plots, the lines in the boxes indicate median values; the upper and lower lines of the boxes indicate the 25th and 75th percentiles, respectively; and the upper and lower whiskers represent the 90th and 10th percentiles, respectively.

supernatant (figure 5*A* and 5*B*). These results suggest that the infectivity (or replication ability) of HBV with hypermutated genomes is very poor. It is possible that the inoculum contained less abundantly mutated genomes. To test this, we cloned and sequenced 72 clones of 217-bp DNA fragments amplified at a denaturation temperature of 95°C. Of 72 clones obtained from the inoculum, we found 1 clone with 8 G-to-A substitutions, 1 clone with 5 substitutions, 2 clones with 3 substitutions, and 1 clone with 1 substitution (figure 5*C*). In contrast, 1 of the 72 clones obtained from the mouse serum had 1 G-to-A substitution. If G-to-A substitutions were excluded, the only other nucleotide substitution observed in the 144 clones sequenced was a single C-to-T substitution.

DISCUSSION

In a previous study, we found that the majority of serum samples obtained from HBV-infected patients contained a small number of hypermutated genomes [27]. Recently, we developed a method (TaqMan 3D-PCR) to measure small numbers of hypermutated genomes [28]. Using this method, we reported dual antiviral effects for APOBEC3G, namely induction of hypermutation and reduction of viral replication. We also reported that IFN increased the transcription of APOBEC3G and enhanced the effect of the protein in vitro [28]. Other investigators also showed that IFN enhances the action of APOBEC proteins against HIV [18–21]. It is thus assumed that the antiviral effect of APOBEC proteins should be enhanced by IFN and other cytokines in vivo.

In the present study, we showed that an increase in ALT level accompanied by an increase in the number of hypermutated genomes was associated with reduction in the plasma HBV DNA level. In contrast, no decrease in HBV DNA level was observed if the increase in ALT level occurred in the absence of an increase in the number of hypermutated genomes. It is difficult to know which of the dual antiviral effects of APOBEC3G (or other APOBEC proteins) reduced the viral level. It is also impossible to estimate the importance of APOBEC proteins in this reduction. However, it is clear that the increase in the number of hypermutated genomes of HBV correlates with activation of the host antiviral defense against HBV.

We also demonstrated that exacerbations of HBV infection associated with a marked increase in the number of hypermutated genomes were associated not only with a decrease in the plasma HBV DNA level but also with clearance of e antigen.

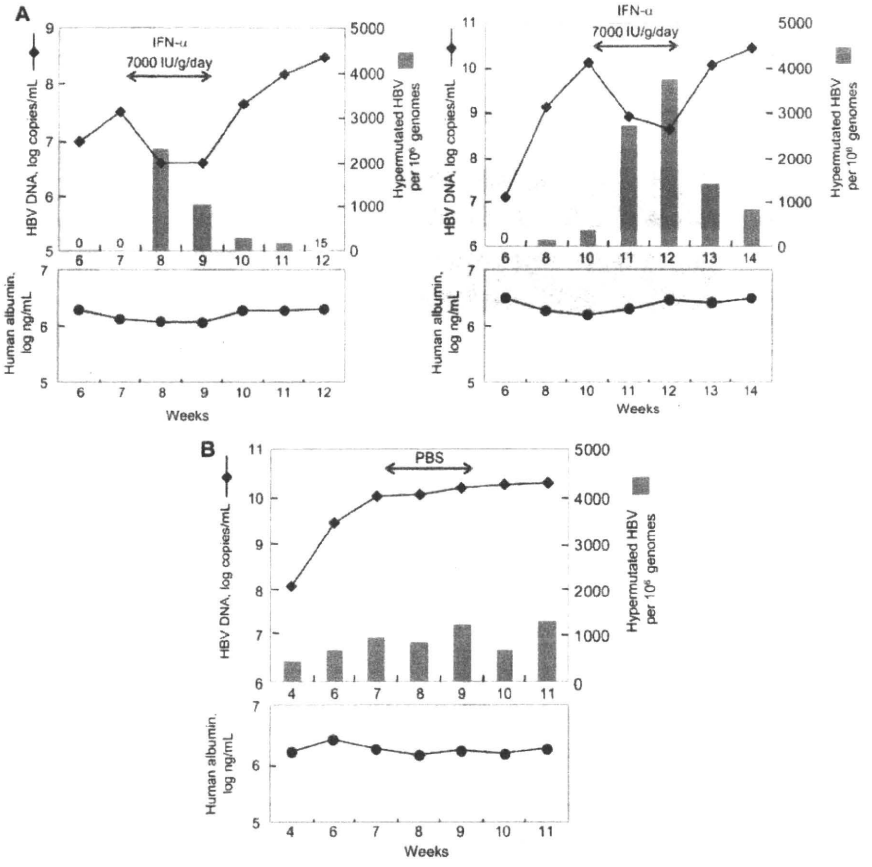

Figure 4. Effect of interferon (IFN)–α therapy on hepatitis B virus (HBV) hypermutation in HBV-infected, human hepatocyte–chimeric mice. Two chimeric mice *(A)* were inoculated with recombinant wild-type HBV produced by transfected HepG2 cells; 10 weeks later, after confirmation of high-level HBV viremia, they were treated with IFN-α at 7000 IU/g/day for 14 days, by intramuscular injection. *Upper panels* in both parts of *A*, serum HBV DNA levels and the number of hypermutated genomes; *lower panels* in both parts of *A*, human serum albumin concentrations. Note that the albumin levels are stable during IFN-α therapy. A control mouse *(B)* was inoculated with recombinant wild-type HBV produced by transfected HepG2 cells and treated with phosphate-buffered saline (PBS). Upper and lower panels of *B* show the same information as in *A*.

Furthermore, all exacerbations followed by seroconversion to positivity for antibody against e antigen were associated with a marked increase in the number of hypermutated genomes. Clearance of e antigen often results from a G-to-A nucleotide substitution at the first position of a 5'-GGGG stretch in the precore coding sequence (the G1896A mutation). Because this substitution (changing TGGGG to TAGGG) is in agreement with the dinucleotide pattern preferentially edited by APOBEC3G, one might assume that G-to-A substitution in this region could be caused by this enzyme and is related to the clearance of e antigen. However, we observed that hypermutation was induced in only some genomes, whereas the majority of genomes were unaffected. Thus, it seems unlikely that APOBEC proteins play a role in seroconversion to positivity for antibody against e antigen, although it is still possible that the 5'-GGGG stretch in the precore region is the preferred editing site for the enzyme. Importantly, such substitution of the 5'-GGGG stretch should result in the occurrence of multiple stop codons (TAG, TGA, and TAA) in HBV genomes, as we observed and reported in our previous study [28], which makes the replication of mutated genomes impossible.

In the present study, we did not observe any increase in the number of hypermutated genomes during IFN therapy in some patients. This finding is discrepant from the results of previous in vitro experiments that showed increased numbers of hypermutated genomes after the application of IFN [28]. Interestingly, our experimental results also showed the induction of APOBEC3G gene expression, an increase in the number of hypermutated genomes, and a reduction of plasma HBV DNA level in 2 human hepatocyte–chimeric mice treated with IFN (figure 4). What is the reason for the lack of increase in hypermutation in some IFN-treated patients? We usually administer IFN to patients who have high ALT levels. The patients in this study had abnormal ALT levels prior to treatment with IFN—that is, their livers were inflamed, and the levels of many cytokines produced by the immune cells in the liver were already high. We presume that the effect of these elevated cytokine levels masked the effect of the IFN we administered. It could also be argued that the effect

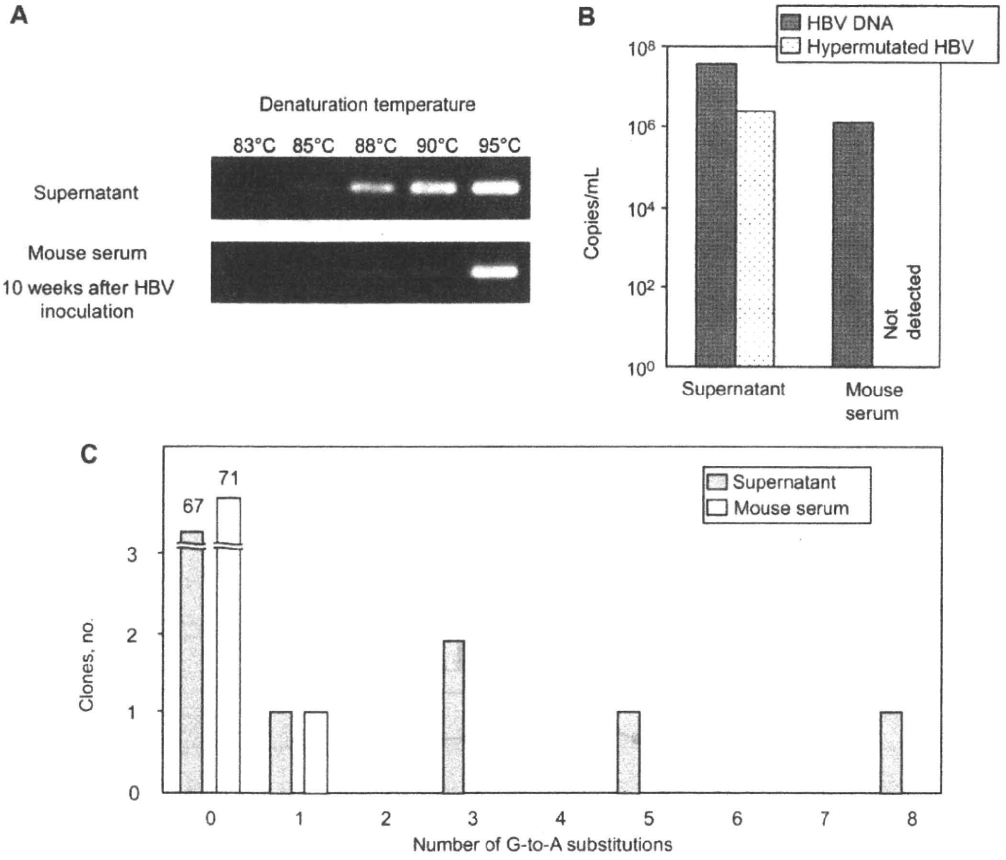

Figure 5. Results for a human hepatocyte–chimeric mouse inoculated with hepatitis B virus (HBV) produced by HepG2 cells transfected with an equal amount (5 μg each) of HBV and apolipoprotein B messenger RNA editing enzyme, catalytic polypeptide–like 3G plasmids. The inoculum contained ~6.25% hypermutated genomes. A serum sample was obtained 10 weeks after the inoculation. *A*, HBV DNA was amplified by polymerase chain reaction (PCR) that used different denaturation temperatures and run on 2% agarose gel. *B*, Quantitative measurement of HBV DNA and hypermutated DNA in the inoculum and mouse serum. *C*, Number of G-to-A substitutions found in each of 72 clones obtained from products of PCR of culture supernatant or mouse serum.

observed in mice represents the absence of the immune response in mice, whereas the lack of a clear response to IFN in the study patients was the result of the complex immune response in human beings. Alternatively, the concentrations of IFN in treated patients might be lower than those used for the cell culture or the chimeric mice. Although we did not perform this analysis in the present study, it would be interesting to determine the expression levels of APOBEC proteins and IFN-stimulated genes in the liver of IFN-treated patients.

The present study showed that the number of hypermutated genomes increased during some increases in ALT level, probably as a result of IFN-activated APOBEC proteins and other cytokines in patients with chronic hepatitis B. However, the number of hypermutated genomes was very small, only 28,378 in 10^6 HBV genomes at most (figure 1*A*). Because it was possible that the less abundantly hypermutated genomes were not detected (i.e., that genomes with only 1 or 2 G-to-A substitutions were not amplified by 3D-PCR), cloning and sequencing were performed to detect such genomes. However, the number of genomes containing G-to-A substitutions was still low (5 [6.9%] of 72 clones), even in the culture medium of HepG2 cells cotransfected with APOBEC3G and HBV (figure 5*C*). This means that the number of genomes with only a small number of G-to-A substitution was not high, suggesting that only selected DNA molecules were heavily mutated while the remaining DNA was not. Does this mean that the effect of APOBEC proteins in antiviral defense is trivial in patients with chronic HBV infection? It is a possible that the heavily deaminated genomes are an easy target for uracil DNA glycocylase. Although the dual antiviral effects of APOBEC proteins are currently known to reduce the amount of HBV, the importance and magnitude of APOBEC proteins with respect to in vivo virus reduction should be investigated further.

Treatment of patients with chronic HBV infection has improved with the advent of new nucleoside and nucleotide analogues. However, reactivation of HBV and flare-ups of hepatitis are often seen in patients who stop such therapy. Furthermore, hepatitis B surface antigen clearance is rare in patients treated

with these antiviral drugs. On the other hand, most patients with chronic HBV infection achieve sufficient viral suppression and disease quiescence through immunological suppression of the virus. As we showed in this study, the immunological suppression of HBV is much stronger than that achieved with IFN therapy, but it is often transient. It is thus necessary to clarify the mechanism of transient immune response and to develop treatment that produces persistent suppression of HBV. Quantitative measurement of hypermutated genomes should be useful in monitoring the immune response in this context.

Acknowledgments

We thank Rie Akiyama, Miyuki Matsushita, and Yoshiko Seo for excellent technical assistance and Yoshiko Nakata for secretarial assistance.

References

1. Wright TL, Lau JYN. Clinical aspects of hepatitis B virus infection. Lancet **1993**; 342:1340–4.
2. Ganem D, Prince AM. Hepatitis B virus infection: natural history and clinical consequences. N Engl J Med **2004**; 350:1118–29.
3. Bruix J, Llovet JM. Hepatitis B virus and hepatocellular carcinoma. J Hepatol **2003**; 39(Suppl 1):S59–63.
4. Sheehy AM, Gaddis NC, Choi JD, Malim MH. Isolation of a human gene that inhibits HIV-1 infection and is suppressed by the viral Vif protein. Nature **2002**; 418:646–50.
5. Mangeat B, Turelli P, Caron G, Friedli M, Perrin L, Trono D. Broad antiretroviral defence by human APOBEC3G through lethal editing of nascent reverse transcripts. Nature **2003**; 424:99–103.
6. Zhang HYB, Pomerantz RJ, Zhang C, Arunachalam SC, Gao L. The cytidine deaminase CEM15 induces hypermutation in newly synthesized HIV-1 DNA. Nature **2003**; 424:94–8.
7. Lecossier D, Bouchonnet F, Clavel F, Hance AJ. Hypermutation of HIV-1 DNA in the absence of the Vif protein. Science **2003**; 300:1112.
8. Harris RS, Bishop KN, Sheehy AM, et al. DNA determination mediates innate immunity to retroviral infection. Cell **2003**; 113:803–9.
9. Liu B, Yu X, Luo K, Yu Y, Yu XF. Influence of primate lentiviral vif and proteasome inhibitors on human immunodeficiency virus type 1 virion packaging of APOBEC3G. J Virol **2004**; 78:2072–81.
10. Mehle A, Strack B, Ancuta P, Zhang C, McPike M, Gabuzda D. Vif overcomes the innate antiviral activity of APOBEC3G by promoting its degradation in the ubiquitin-proteasome pathway. J Biol Chem **2004**; 279:7792–8.
11. Marin M, Rose KM, Kozak SL, Kabat D. HIV-1 Vif protein binds the editing enzyme APOBEC3G and induces its degradation. Nat Med **2003**; 9:1398–403.
12. Stopak K, de Noronha C, Yonemoto W, Greene WC. HIV-1 Vif blocks the antiviral activity of APOBEC3G by impairing both its translation and intracellular stability. Mol Cell **2003**; 12:591–601.
13. Zack JA, Arrigo SJ, Weitsman SR, Go AS, Haislip A, Chen IS. HIV-1 entry into quiescent primary lymphocytes: molecular analysis reveals a labile, latent viral structure. Cell **1990**; 61:213–22.
14. Korin YD, Zack JA. Progression to the G1b phase of the cell cycle is required for completion of human immunodeficiency virus type 1 reverse transcription in T cells. J Virol **1998**; 72:3161–8.
15. Pierson TC, Zhou Y, Kieffer TL, Ruff CT, Buck C, Siliciano RF. Molecular characterization of preintegration latency in human immunodeficiency virus type 1 infection. J Virol **2002**; 76:8518–31.
16. Stevenson M, Stanwick TL, Dempsey MP, Lamonica CA. HIV-1 replication is controlled at the level of T cell activation and proviral integration. EMBO J **1990**; 9:1551–60.
17. Chiu YL, Soros VB, Kreisberg JF, Stopak K, Yonemoto W, Greene WC. Cellular APOBEC3G restricts HIV-1 infection in resting CD4$^+$ T cells. Nature **2005**; 435:108–14.
18. Tanaka Y, Marusawa H, Seno H, et al. Antiviral protein APOBEC3G is induced by interferon-alpha stimulation in human hepatocytes. Biochem Biophys Res Commun **2006**; 341:314–9.
19. Peng G, Lei KJ, Jin W, Greenwell-Wild T, Wahl SM. Induction of APOBEC3 family proteins, a defensive maneuver underlying interferon-induced anti-HIV-1 activity. J Exp Med **2006**; 203:41–6.
20. Bonvin M, Achermann F, Greeve I, et al. Interferon-inducible expression of APOBEC3 editing enzymes in human hepatocytes and inhibition of hepatitis B virus replication. Hepatology **2006**; 43:1364–74.
21. Chen K, Huang J, Zhang C, et al. Alpha interferon potently enhances the anti-human immunodeficiency virus type 1 activity of APOBEC3G in resting primary CD4 T cells. J Virol **2006**; 80:7645–57.
22. Newman EN, Holmes RK, Craig HM, et al. Antiviral function of APOBEC3G can be dissociated from cytidine deaminase activity. Curr Biol **2005**; 15:166–70.
23. Navarro F, Bollman B, Chen H, et al. Complementary function of the two catalytic domains of APOBEC3G. Virology **2005**; 333:374–86.
24. Nguyen DH, Gummuluru S, Hu J. Deamination-independent inhibition of hepatitis B virus reverse transcription by APOBEC3G. J Virol **2007**; 81:4465–72.
25. Gunther S, Sommer G, Plikat U, Iwanska A, WainHobson S, Will H, et al. Naturally occurring hepatitis B virus genomes bearing the hallmarks of retroviral G→A hypermutation. Virology **1997**; 235:104–8.
26. Suspene R, Guetard D, Henry M, Sommer P, Wain-Hobson S, Vartanian JP. Extensive editing of both hepatitis B virus DNA strands by APOBEC3 cytidine deaminases in vitro and in vivo. Proc Natl Acad Sci U S A **2005**; 102:8321–6.
27. Noguchi C, Ishino H, Tsuge M, et al. G to A hypermutation of hepatitis B virus. Hepatology **2005**; 41:626–33.
28. Noguchi C, Hiraga N, Mori N, et al. Dual effect of APOBEC3G on hepatitis B virus. J Gen Virol **2007**; 88:432–40.
29. Desmet VJ, Gerber M, Hoofnagle JH, Manns M, Scheuer PJ. Classification of chronic hepatitis: diagnosis, grading and staging. Hepatology **1994**; 19:1513–20.
30. Norder H, Courouce AM, Magnius LO. Complete genomes, phylogenetic relatedness, and structural proteins of 6 strains of the hepatitis-B virus, 4 of which represent 2 new genotypes. Virology **1994**; 198:489–503.
31. Tsuge M, Hiraga N, Takaishi H, et al. Infection of human hepatocyte chimeric mouse with genetically engineered hepatitis B virus. Hepatology **2005**; 42:1046–54.
32. Tateno C, Yoshizane Y, Saito N, et al. Near completely humanized liver in mice shows human-type metabolic responses to drugs. Am J Pathol **2004**; 165:901–12.

Toxicology and Applied Pharmacology 237 (2009) 119–126

Contents lists available at ScienceDirect

Toxicology and Applied Pharmacology

journal homepage: www.elsevier.com/locate/ytaap

CYP1A1 and CYP1A2 expression: Comparing 'humanized' mouse lines and wild-type mice; comparing human and mouse hepatoma-derived cell lines

Shigeyuki Uno [a], Kaori Endo [a], Yuji Ishida [b], Chise Tateno [b], Makoto Makishima [a], Katsutoshi Yoshizato [b], Daniel W. Nebert [c,*]

[a] Department of Biochemistry, Nihon University School of Medicine, 30-1 Oyaguchikami-cho, Itabashi-ku, Tokyo 173-8610, Japan
[b] PhenixBio Co., Ltd., 3-4-1 Kagamiyama, Higashihiroshima, Hiroshima 739-0046, Japan
[c] Department of Environmental Health and Center for Environmental Genetics (CEG) University of Cincinnati Medical Center, P.O. Box 670056, Cincinnati OH 45267-0056, USA

ARTICLE INFO

Article history:
Received 17 November 2008
Revised 10 February 2009
Accepted 2 March 2009
Available online 10 March 2009

Keywords:
Cytochrome P450 1 (*CYP1*) genes
Bacterial artificial chromosome (BAC)
hCYP1A1_1A2_Cyp1a1/1a2(−/−)
BAC-transgenic mouse line
uPA/SCID chimeric mouse line
carrying human hepatocytes
Human risk assessment
Western immunoblot
Benzo[*a*]pyrene hydroxylase,
ethoxyresorufin *O*-deethylase,
acetanilide 4-hydroxylase
and methoxyresorufin *O*-demethylase
as CYP1A1 and CYP1A2 substrates
2,3,7,8-Tetrachlorodibenzo-*p*-dioxin
(TCDD, dioxin) as P450 inducer
Mouse Hepa-1c1c7 cell culture
Human HepG2 cell culture

ABSTRACT

Human and rodent cytochrome P450 (**CYP**) enzymes sometimes exhibit striking species-specific differences in substrate preference and rate of metabolism. Human risk assessment of CYP substrates might therefore best be evaluated in the intact mouse by replacing mouse *Cyp* genes with human *CYP* orthologs; however, how "human-like" can human gene expression be expected in mouse tissues? Previously a bacterial-artificial-chromosome-transgenic mouse, carrying the human *CYP1A1_CYP1A2* locus and lacking the mouse *Cyp1a1* and *Cyp1a2* orthologs, was shown to express robustly human dioxin-inducible CYP1A1 and basal versus inducible CYP1A2 (mRNAs, proteins, enzyme activities) in each of nine mouse tissues examined. Chimeric mice carrying humanized liver have also been generated, by transplanting human hepatocytes into a urokinase-type plasminogen activator(+/+)_severe-combined-immunodeficiency (*uPA/SCID*) line with most of its mouse hepatocytes ablated. Herein we compare basal and dioxin-induced CYP1A mRNA copy numbers, protein levels, and four enzymes (benzo[*a*]pyrene hydroxylase, ethoxyresorufin *O*-deethylase, acetanilide 4-hydroxylase, methoxyresorufin *O*-demethylase) in liver of these two humanized mouse lines versus wild-type mice; we also compare these same parameters in mouse Hepa-1c1c7 and human HepG2 hepatoma-derived established cell lines. Most strikingly, mouse liver CYP1A1-specific enzyme activities are between 38- and 170-fold higher than human CYP1A1-specific enzyme activities (per unit of mRNA), whereas mouse versus human CYP1A2 enzyme activities (per unit of mRNA) are within 2.5-fold of one another. Moreover, both the mouse and human hepatoma cell lines exhibit striking differences in CYP1A mRNA levels and enzyme activities. These findings are relevant to risk assessment involving human CYP1A1 and CYP1A2 substrates, when administered to mice as environmental toxicants or drugs.

Introduction

The human and mouse genomes comprise 57 and 102 protein-coding cytochrome P450 (**CYP**) genes, respectively, each divided into 18 families (Nelson et al., 2004; Nebert et al., 2004; Nebert and Dalton, 2006). The mammalian *CYP1* gene family encodes three enzymes in both human and mouse—CYP1A1, CYP1A2 and CYP1B1. While the *CYP1A* and *CYP1B* subfamily ancestors diverged from one another ~480 million years ago, *CYP1A2* arose as a duplication event from the *CYP1A1* gene about 420 million years ago. Thus, land animals (including birds) carry both *CYP1A1* and *CYP1A2*; on the other hand, fish genomes do not contain the *CYP1A2* gene (Nelson et al., 1996).

It was originally noted that alteration of a single amino-acid in a CYP protein could change dramatically its catalytic activity from coumarin to testosterone hydroxylation (Lindberg and Negishi, 1989). Similarly, numerous other examples have shown that human and rodent CYP1A2 orthologs, having important amino-acid differences, can display striking species-specific variability in the rates by which certain substrates are metabolized (Turesky, 2005). For example, human and mouse CYP1A2 differ by 3- to 7-fold in catalyzing ethoxyresorufin *O*-deethylation (Aoyama et al., 1989) and uroporphyrinogen oxidation (Nichols et al., 2003).

It therefore can be difficult to extrapolate toxicity or cancer data from rodent studies to human risk assessment. For this reason, we and others have generated "humanized" *hCYP1A1_1A2* transgenic lines in which either mouse *Cyp1a1* or *Cyp1a2* (Jiang et al., 2005; Cheung et al., 2005; Derkenne et al., 2005) or both mouse *Cyp1a1* and *Cyp1a2* (Dragin et al., 2007; Shi et al., 2008) orthologs are

* Corresponding author. Fax: +1 513 558 0974.
E-mail address: dan.nebert@uc.edu (D.W. Nebert).

0041-008X/$ - see front matter © 2009 Published by Elsevier Inc.
doi:10.1016/j.taap.2009.03.001

ablated. In addition, a global approach for making a humanized mouse has been developed by transplanting human hepatocytes into the urokinase-type plasminogen activator(+/+)_severe-combined-immunodeficiency (*uPA/SCID*) mouse, which otherwise is immunodeficient and undergoes liver failure; these chimeric mice no longer develop liver failure, but rather the mouse liver comprises >70% human hepatocytes that propagate successfully and retain normal pharmacological functions such as drug metabolism (Tateno et al., 2004; Katoh et al., 2008). Eight human P450s (CYP1A2, 2A6, 2C8, 2C9, 2C19, 2D6, 3A4, 3A5), 35 other Phase I enzymes, and four classes of Phase II conjugating enzymes (UDP glucuronosyltransferases, glutathione *S*-transferases, *N*-acetyltransferases, and sulfotransferases) have been shown to be functional in chimeric mice (Katoh et al., 2008). Because each chimeric mouse will reflect the liver profile and genetic makeup of the human donor's hepatocytes, interindividual and ethnic differences in drug metabolism will undoubtedly exist. Nevertheless, variations of xenobiotic-metabolizing enzymes as well as other enzymes, receptors, transporters, transcription factors, and any other drug target located in human liver—might effectively be studied in such chimeric mouse lines.

Mammalian CYP1A1 basal mRNA is known to be negligible, resulting in no detectable CYP1A1 protein in any tissue, whereas basal levels of CYP1A2 mRNA and protein are relatively high in liver but generally low (protein undetectable on Western immunoblot) in nonhepatic tissues; induction by a CYP1 inducer such as chemicals in cigarette smoke or 2,3,7,8-tetrachlorodibenzo-*p*-dioxin (**TCDD**; **dioxin**) increases CYP1A1 and CYP1A2 mRNA and protein levels (Eaton et al., 1995; Nebert et al., 2004). Recently, two humanized *CYP1A1_1A2* lines were compared with C57BL/6J (**B6**) inbred mice with regard to expression of CYP1A1 and CYP1A2 mRNA levels following TCDD pretreatment. Maximally-induced mRNA concentrations of mouse CYP1A1 were ~10 times higher in liver and lung and ~100-fold greater in kidney than those of human CYP1A1 (Shi et al., 2008). On the other hand, maximally-induced mRNA levels of mouse CYP1A2 in liver were <2-fold higher than those of human CYP1A2. Maximally-induced mRNA levels of human CYP1A2 in liver were ~12 times higher than those of human CYP1A1, whereas maximally-induced mRNA levels of mouse CYP1A2 in liver were ~3-fold greater than those of mouse CYP1A1 (Shi et al., 2008).

These data caused us to query how "physiologically" relevant these human mRNA levels might be, in the intact mouse. Do these humanized mouse lines actually reflect "average" *CYP1A1* and *CYP1A2* gene expression that might be expected among individuals in a human population, or is this expression abnormally low or high? One should be able to shed some light on this, by comparing precise copy numbers of basal and TCDD-induced CYP1A1 and CYP1A2 mRNA (combined with quantification of protein levels and enzyme assays) in the humanized mouse lines versus wild-type mice.

Those who oppose the use of laboratory animals, and recommend instead that everyone utilize cells in culture, often declare that studies with cultured cell lines can provide information that would accurately reflect what is found in the intact animal. We therefore have compared the above-mentioned CYP1A1 and CYP1A2 parameters in liver from the humanized mouse lines and wild-type mice with those in human versus mouse hepatoma-derived established cell culture lines. The present study addresses these questions. Answering these questions should be beneficial, before launching into human risk assessment studies using such humanized mouse lines.

Material and methods

Mice. C57BL/6J (B6) mice were purchased from The Jackson Laboratory (Bar Harbor, ME). Development of the humanized *hCYP1A1_1A2_Cyp1a1/1a2(−/−)-Ahr^{b1}* transgenic line has been detailed (Dragin et al., 2007). Chimeric mice bearing human hepatocytes were generated using *uPA(+/+)/SCID* mice as the host (Giannini et al., 2003) and characterized (Tateno et al., 2004; Katoh et al., 2008); their human hepatocyte-replacement rates were between 73% and 83%. All experiments involving mice adhered to the Guidelines for Animal Experiments and Use Committee of the Nihon University School of Medicine.

Treatment of mice. Mice were treated with intraperitoneal TCDD (25 μg/kg for 24 h), versus corn oil vehicle alone for untreated. At least three groups ($N = 3$ each time) were studied to ensure reproducibility.

Cell cultures and treatment. The human HepG2 established cell line was derived from a hepatoblastoma (Dearfield et al., 1983). The mouse Hepa-1c1c7 line was derived from a C57L/J hepatoma (Bernhard et al., 1973). Cultured cells were treated with 10 nM TCDD for 24 h before total RNA isolation.

Reverse transcription. Total RNAs from samples were prepared by the acid guanidine thiocyanate-phenol/chloroform method (Tavangar et al., 1990). The cDNAs were synthesized using the ImProm-II Reverse Transcription system (Promega, Madison, WI) (Inaba et al., 2007).

Quantitative real-time PCR (qRT-PCR). We used the primers listed in Table 1. The qRT-PCR was performed in an ABI PRISM 7000 Sequence Detection System™ (Applied Biosystems), using Power SYBR Green PCR Master Mix (Applied Biosystems). Individual CYP1 mRNA abundance was determined, using the standard-curve method (from 10^1 to 10^8 copies/μL), as previously described by K. Livak (PE-ABI; Sequence Detector User; Bulletin #2) (Winer et al., 1999). Each sample was normalized to mouse glyceraldehyde-3-phosphate dehydrogenase (**GAPDH**) mRNA.

CYP1A mRNA copy numbers. Transcripts from the human *CYP1A1* and *CYP1A2* and the mouse *Cyp1a1* and *Cyp1a2* genes were quantified by fitting qRT-PCR data to a curve generated from cloned RNAs (cRNAs) for each CYP1. Briefly described, templates for cRNA synthesis were produced by PCR on cDNA constructs from each CYP1A cDNA that had been cloned into pcDNA3.1(+) (Invitrogen), using T7 RiboMAX™ Express Large-Scale RNA Production System (Promega) (Uno et al., 2006). The cRNAs were used to generate a standard curve in the PCR reactions from which mRNA copy numbers from qRT-RNA measurements could be extrapolated.

Western immunoblot analysis. Mice were euthanized by carbon dioxide asphyxiation followed by cervical dislocation. The liver was excised, and microsomes were prepared as previously described (Dalton et al., 2000). Protein concentrations were determined by the bicinchoninic acid method (Pierce Chemical Co.; Rockford, IL), according to details provided by the manufacturer. Microsomal proteins were separated on sodium dodecylsulfate (0.1%)–polyacrylamide (12%) minigels. Separated proteins were transferred to nitrocellulose membranes. Western immunoblot analysis was performed using goat polyclonal anti-rat CYP1A1/1A2 antibody; this antibody (Daiichi Pure Chemicals, Tokyo, Japan) recognizes both the human and mouse CYP1A1 and CYP1A2 proteins. We used alkaline phosphatase-conjugated secondary antibodies (Kirkegaard Perry Lab., Gaithersburg, MD) and the Alkaline

Table 1
Primer pairs used in qRT-PCR.

Gene	Forward primer	Reverse primer
hCYP1A1	5′-AAGGGGCGTTGTGTCTTTGT-3′	5′-ATACACTTCCGCTTGCCCAT-3′
hCYP1A2	5′-ACAAGGGACACAACGCTGAA-3′	5′-AGGGCTTGTTAATGGCAGTG-3′
mCyp1a1	5′-CCTCATGTACCTGGTAACCA-3′	5′-AAGGATGAATGCCGGAAGGT-3′
mCyp1a2	5′-AAGACAATGGCGGTCTCATC-3′	5′-GACGGTCAGAAAGCCGTGGT-3′
mGapdh	5′-TGCACCACCAACTGCTTAG-3′	5′-GATGCAGGGATGATGTTC-3′

h, human; m, mouse.

Phosphatase Conjugate Substrate Kit™ (Bio-Rad Lab., Hercules, CA), with exposure times ranging from 5 to 10 min.

Enzyme assays. Determination of microsomal BaP hydroxylase (Nebert and Gelboin, 1968) and ethoxyresorufin *O*-deethylase (**EROD**) (Burke et al., 1977) activities principally represent CYP1A1 activity. Acetanilide 4-hydroxylase (Shertzer et al., 2001) and methoxyresorufin *O*-demethylase (**MROD**) (Berthou et al., 1992; Hamm et al., 1998; Shertzer et al., 2001) activities principally (but not exclusively) represent CYP1A2 activity. These enzymes were assayed by the methods cited. Although the MROD spectrophotofluororometric assay is sensitive and reliable, it has been demonstrated (Hamm et al., 1998) that the MROD assay is not the most suitable for estimating CYP1A2 activity. In *Cyp1a2(−/−)* knockout mice, it was shown that hepatic MROD activity was increased 70-fold by TCDD treatment, indicating that other TCDD-inducible enzymes contribute to inducible MROD activity. In contrast, acetanilide 4-hydroxylase activity in *Cyp1a2(−/−)* knockout mice was induced only 2-fold by dioxin (Shertzer et al., 2001), suggesting that it is by far the preferred enzyme activity for estimating CYP1A2 catalytic expression.

Biohazard precaution. TCDD is highly toxic and regarded as a likely human carcinogen. All personnel were instructed in safe handling procedures. Lab coats, gloves and masks were worn at all times, and contaminated materials were collected separately for disposal by the Hazardous Waste Unit or by independent contractors. TCDD-treated mice were housed separately, and their carcasses regarded as contaminated biological materials. TCDD-treated cells in culture, and culture medium from these cells, were also regarded as contaminated biological materials.

Statistical analysis. Statistical significance between groups was determined by analysis-of-variance among groups and Student's *t*-test between groups. All assays were performed in duplicate or triplicate, and repeated at least twice. Statistical analyses were also carried out with the use of SAS® statistical software (SAS Institute Inc.; Cary, NC) and Sigma Plot (Systat Software, Inc., Point Richmond, CA).

Results and discussion

Factors affecting CYP expression

In a previous study of the entire gastrointestinal tract (Uno et al., 2008), large differences in basal but especially inducible CYP1A1 and CYP1A2 mRNA and protein levels were seen. This variability appears to depend on the route-of-administration and the target organ being studied: oral versus intraperitoneal administration of TCDD or BaP can drastically alter CYP1 mRNA levels in various cell types of the intestine, from tongue to colon (Uno et al., 2008). In two studies comparing humanized mice with wild-type controls (Dragin et al., 2007; Shi et al., 2008), large differences were also observed in human CYP1A1 or CYP1A2 mRNA, compared with mouse CYP1A1 or CYP1A2 mRNA. In the chimeric *uPA/SCID* humanized mouse, although CYP1A1 was not studied, large variability in CYP1A2 expression has also been seen (Katoh et al., 2008).

Reasons for differences in human transgene expression in humanized mouse tissues include: [a] genotype of the volunteer from whom the BAC library was derived (Jiang et al., 2005) or from whose hepatocytes were infused into a *uPA(+/+)/SCID* mouse (Katoh et al., 2008; [b] chromosomal location of the randomly inserted BAC transgene affecting transgene expression, *i.e.* the "neighborhood effect" (Bedell et al., 1996; Milot et al., 1996; Olson et al., 1996; Muller et al., 2001); [c] genetic background (modifier genes) of a particular inbred strain that can influence transgene expression (Bonyadi et al., 1997; Cranston and Fishel, 1999; Bennett et al., 2000); and [d] a BAC containing the human gene(s) (Jiang et al., 2005; Cheung et al., 2005) which does not include *trans*-regulatory, or all of the *cis*-regulatory, sites needed for "normal" expression of the transgene(s) in each mouse tissue or cell type studied.

Comparison of human versus mouse CYP1A1 mRNA levels in liver

Fig. 1A compares human and mouse CYP1A1 mRNA copy numbers in the *hCYP1A1_1A2_Cyp1a1/1a2(−/−)* line, B6 wild-type mice containing no human transgenes, chimeric *uPA/SCID* mice (**chimera**), and *uPA(+/+)/SCID* control mice containing no human hepatocytes (*uPA/SCID* mice). Human basal CYP1A1 mRNA levels in the liver of *hCYP1A1_1A2* and chimeric mice were quite low, having $\sim 1.3 \times 10^7$ and $\sim 1.2 \times 10^7$ transcript copy numbers (per μg total RNA), respectively; both were strikingly increased by TCDD to $\sim 7.3 \times 10^9$ and $\sim 2.0 \times 10^9$ copy numbers, respectively.

Mouse basal CYP1A1 mRNA levels in B6, chimeric, and *uPA/SCID* mice (Fig. 1A) were also quite low ($\sim 1.8 \times 10^6$, $\sim 1.7 \times 10^6$, and 1.0×10^6 copy numbers, respectively), but all were dramatically induced by TCDD to $\sim 2.5 \times 10^8$, $\sim 8.0 \times 10^7$, and $\sim 1.5 \times 10^8$ copy numbers, respectively. As expected, no human CYP1A1 mRNA was detected in B6 or *uPA/SCID* mice, and no mouse CYP1A1 mRNA was detected in the *hCYP1A1_1A2_Cyp1a1/1a2(−/−)* line.

Comparison of human versus mouse CYP1A2 mRNA levels in liver

Human basal CYP1A2 mRNA levels in *hCYP1A1_1A2_Cyp1a1/1a2(−/−)* and chimeric mice (Fig. 1B) were low ($\sim 2.6 \times 10^8$ and $\sim 0.89 \times 10^8$ transcript copy numbers, respectively). Both were significantly elevated by TCDD to $\sim 9.7 \times 10^8$ and $\sim 7.7 \times 10^8$ copy numbers, respectively.

Mouse basal CYP1A2 mRNA concentrations in B6, chimeric, and *uPA/SCID* mice were also low ($\sim 2.2 \times 10^8$, $\sim 0.16 \times 10^8$ and $\sim 1.2 \times 10^8$ copy numbers, respectively); all three were significantly induced by TCDD to $\sim 4.2 \times 10^9$, $\sim 0.73 \times 10^9$, and 2.8×10^9 copy numbers, respectively (Fig. 1B). As expected, no human CYP1A2 mRNA was detected in B6 and *uPA/SCID* mice, and no mouse CYP1A2 mRNA was detected in the *hCYP1A1_1A2_Cyp1a1/1a2(−/−)* line.

Comparison of human versus mouse CYP1A1 and CYP1A2 mRNA levels

It should be noted that the basal expression levels of human and mouse CYP1A2 mRNA ($1–3 \times 10^8$ copy numbers) were much higher (Fig. 1) than those of CYP1A1 mRNA ($\sim 10^7$ copy numbers). This conclusion supports the results of studies long ago (Nebert, 1989; Eaton et al., 1995). The induction of human and mouse CYP1A1 and CYP1A2 mRNAs by TCDD is also well known (Nebert, 1989; Eaton et al., 1995; Nebert et al., 2004).

A previous report (Shi et al., 2008) compared the expression of CYP1A1 and CYP1A2 mRNA in liver between two humanized *CYP1A1_1A2_Cyp1a1/1a2(−/−)* lines and the B6 inbred mouse: maximally-induced mRNA levels of mouse CYP1A1 were described as ~10 times higher than those of human CYP1A1; in contrast, maximally-induced mRNA levels of mouse CYP1A2 were <2-fold higher than those of human CYP1A2 in liver. However, the present study (in which we find a mouse/human induced CYP1A1 ratio of ~0.03 and a mouse/human induced CYP1A2 ratio of ~4) appears not to be consistent with this previous report.

The previous report also found that maximally-induced mRNA levels of human CYP1A2 in liver were ~12 times higher than those of human CYP1A1, whereas maximally-induced mRNA levels of mouse CYP1A2 were ~3-fold greater than those of mouse CYP1A1 (Shi et al., 2008). In the present study, these ratios are 0.13 and 16.8, respectively. These large differences in the calculated ratios clearly reflect the

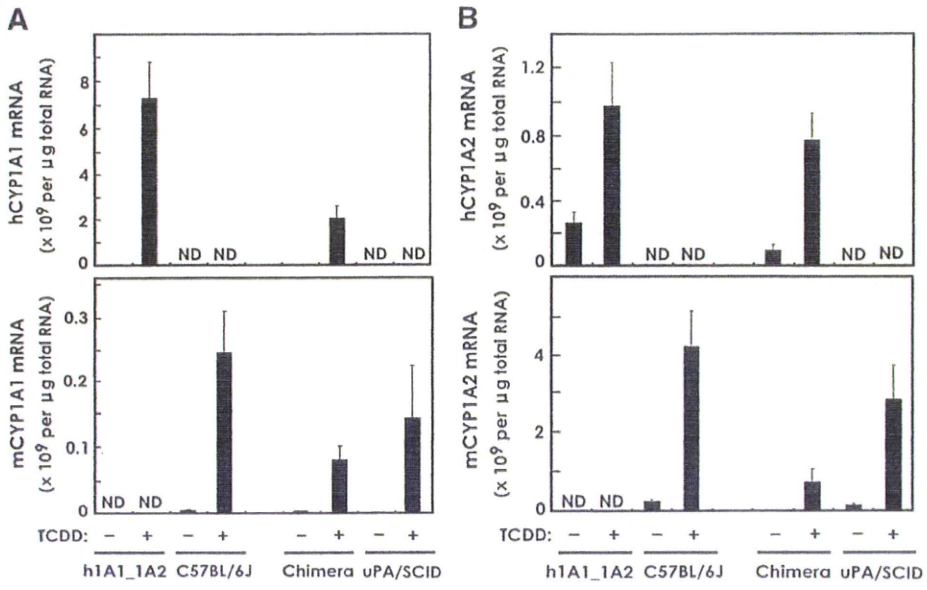

Fig. 1. Human (*upper panels*) versus mouse (*lower panels*) CYP1A1 (A) and CYP1A2 (B) mRNA copy numbers in liver from the *hCYP1A1_1A2_Cyp1a1/1a2(−/−)_Ahr^{b1}* mouse line, B6 inbred mouse, chimeric mouse, and *uPA/SCID* mouse—with, versus without, TCDD pretreatment. When administered, TCDD (25 µg/kg body weight 24 h before killing) was given intraperitoneally. "**ND**" (nondetectable by qRT-PCR) denotes nothing above background, whereas absence of "ND" (detectable, but extremely low by qRT-PCR) denotes something measurable above background. On *Y*-axis: **h**CYP1A1 or **h**CYP1A2 = human mRNA; **m**CYP1A1 or **m**CYP1A2 = mouse mRNA. For this figure and Fig. 4, the method for determining the copy number of mRNA molecules per µg total RNA is given in "Materials & methods". Note the different labels on the *Y*-axes of these figures. *Bars* and *brackets* denote means ± S.E.M., respectively ($N = 3$ independent experiments).

disparity between the "relative values" given in the previous report and the "absolute values" (*i.e.* copy numbers per µg total RNA) in the present study.

Human induced and basal CYP1A2 mRNA copy numbers in chimeric mice were 73–80% lower than those in *uPA/SCID* mice (Fig. 1B). This decrease can easily be explained when the human hepatocyte-replacement rate (73%–83%) is taken into account. This finding supports the notion that human hepatocytes in chimeric mice liver are affected by TCDD independently from mouse hepatocytes, suggesting that human hepatocytes in chimeric mice liver can mimic those in human liver.

The induction rate (Fig. 1) of human CYP1A1 mRNA in the *hCYP1A1_1A2_Cyp1a1/1a2(−/−)* line is quite remarkable (>500-fold), whereas that in chimeric mouse was not nearly as high (~170-fold). In contrast, the induction rate of human CYP1A2 mRNA in *hCYP1A1_1A2_Cyp1a1/1a2(−/−)* mice was ~3.7-fold, whereas that in the chimera was higher (~8.7-fold). These differences in fold-induction could be due to differences in the transcription regulatory regions associated with each of the two genes—if we assume that human and mouse genomic regulatory motifs might differ in their ability to govern these two human transgenes. This might not be a valid assumption, however, because many transcription factors and their DNA-binding motifs are highly conserved among vertebrates and, indeed, in some cases down to the fly, worm and yeast.

The BAC carrying the human *CYP1A1_CYP1A2* locus includes the 23.3-kb bidirectional promoter, plus 56 kb 3′-ward of *CYP1A1* and 86 kb 3′-ward of *CYP1A2* (Jiang et al., 2005). The transgenes in the *hCYP1A1_1A2_Cyp1a1/1a2(−/−)* mouse thus would carry human *cis*-regulatory motifs only within these sequences responsible for TCDD up-regulation, whereas expression of the human *CYP1A1* and *CYP1A2* genes in chimeric mice should be controlled by any and all of the human *cis*- and *trans*-regulatory enhancers in the same way as they are in human liver hepatocytes.

The expression level of mouse CYP1A1 induced mRNA in B6 is comparable to that in *uPA/SCID* mice and might also be comparable to that in chimeric mice when the human hepatocyte-replacement rate is taken into consideration. A similar conclusion might also be reached if one compares the expression levels of mouse induced CYP1A2 mRNA among B6, chimeric, and *uPA/SCID* mice. As a whole, we conclude that the *hCYP1A1_1A2_Cyp1a1/1a2(−/−)* line and the human hepatocyte chimeric mouse show similar expression levels of basal mRNA for the human *CYP1A1* and *CYP1A2* genes. Likewise, there are similar expression levels of TCDD-induced mRNA for these two genes, although their extent of induction is variable.

Comparison of human versus mouse CYP1A1 and CYP1A2 protein levels in liver

Western immunoblots of liver were carried out from the four mouse types, control versus TCDD-pretreated (Fig. 2). The polyvalent antiserum was raised against rat CYP1A1/1A2 and thus is not likely to recognize equally the human and mouse CYP1A1 and CYP1A2 proteins; consequently, a strict quantitative comparison of the human versus mouse orthologous protein concentrations is not possible. This problem has been recognized before and discussed in detail (Jiang et al., 2005).

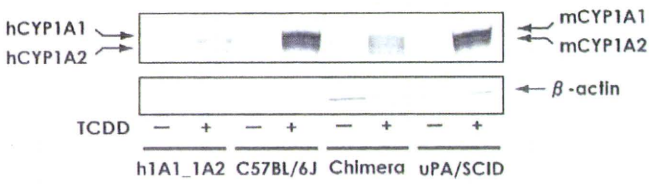

Fig. 2. Western immunoblot analysis of mouse versus human hepatic CYP1A1 and CYP1A2 proteins in the same mouse lines as in Fig. 1, using a polyclonal antibody that recognizes both mammalian CYP1A1 and CYP1A2. TCDD-induced mouse and human CYP1A1 proteins are both ~56.0 kDa, whereas TCDD-induced mouse and human CYP1A2 proteins are both ~54.5 kDa. Lanes 1–2 represent human CYP1A proteins only, whereas lanes 5–6 represent ~78% human CYP1A proteins and ~22% mouse CYP1A proteins. Lanes 3–4 and 7–8 depict only mouse CYP1A proteins. We used β-actin mRNA as a control for standardizing the amount of protein loaded per lane. The amount of microsomal protein (10 µg) loaded per lane was constant for all lanes.